High Steaks: Modeling the Long-Term Temperature Impact of Short- and Long-Lived Greenhouse Gas Emissions from the American Beef Industry

Andy Hur[1], Paige Millis-Wight[2], Leo Valenti[3], Keval Parmar[4], and Steffen E. Eikenberry[5]

[1]Department of Statistics and Data Science, Southern Methodist University
[2,5]School of Mathematical and Statistical Sciences, Arizona State University
[3]Mathematics and Statistics Department, Vassar College
[4]Ira A. Fulton School of Engineering, Arizona State University

July 2024

Abstract

Livestock are a major contributor to climate change via non-CO_2 emissions, namely methane and nitrous oxide. However, the long-term effect of these gases may be poorly resolved using the traditional carbon dioxide-equivalent metric, motivating efforts to quantify livestock's climate impact using either metric-free approaches or alternative metrics. We develop a reduced-complexity climate model for global temperature response to emissions streams of carbon dioxide, which is very long-lived in the atmosphere and shuttles between multiple geophysical compartments; methane, which is short-lived; and nitrous oxide, which has an intermediate half-life. The model is driven by historical emissions through the present, and different representative concentration pathways (RCPs) through the year 2500. The marginal temperature impact of US beef cattle emissions is determined on these background emissions. Cattle emissions are calculated using a continuous-time beef herd model, divided into seven geographic regions, that includes each major system node: Cow/calf on pasture, replacement heifers, stocker cattle, and cattle finished on both high-grain diets in feedlots and on grass pasture. Direct livestock methane and nitrous oxide emissions are estimated at each stage, while emissions from imported feed are also estimated. We find that the effect on temperature perturbation for each region correlates poorly with the traditional carbon dioxide-equivalent metric. Moreover, while methane dominates the shorter-term impact of cattle, it has a more marginal effect on long-term temperature perturbation; N_2O is the dominant influence on warming on centuries-long time-scales. Thus, mitigation efforts should focus on nitrous oxide through improved manure management and optimizing fertilizer use for upstream feed production.

1 Introduction

The need to adapt to the ever-growing problem of climate change exists at all levels of society. The Intergovernmental Panel on Climate Change (IPCC) reaffirmed in its Climate Change 2023 Synthesis Report that human activity, specifically the release of greenhouse gases (GHG), has led to the warming of the Earth. The global temperature has increased by 1.1°C since the pre-industrial era, with an even larger temperature increase over land (1.59°C) than oceans [23]. Phasing out CO_2 emissions and deep reductions in non-CO_2 emissions are necessary to limit future warming and the potential disastrous climate effects associated with more warming [33].

Agriculture is a major contributor to climate altering emissions: The Working Group III of the sixth IPCC report found that agriculture, forestry, and other land use (AFOLU) was responsible for 22% of global emissions in 2019 [10]. A 2012 study found that the global agriculture industry contributed 19-29% percent of worldwide GHG emissions in 2008 [43]. The majority of agricultural emissions are from the cattle industry, due to the large amount of land use for cattle and methane emissions from enteric fermentation. The dairy and, especially, the beef industries, have very high emissions footprints in terms of kg CO_2-equivalent (CO_2e) per kg of product [27].

The three main greenhouse gases released by the beef industry are methane (CH_4), nitrous oxide (N_2O), and carbon dioxide (CO_2). The most common metric for comparing the warming effects of different greenhouse gases is Global Warming Potential (GWP), which compares how much energy a kg of a given GHG absorbs in the atmosphere compared to a kg of CO_2 over a period of time, usually 100 years, and is the basis of the CO_2e metric [38]. However, recent work has suggested that GWP, and emission metrics that aggregate different GHGs in general, can misrepresent the climate effects of short-lived climate pollutants (SLCPs) [26]. This is primarily due to the fact that CO_2 has a very long atmospheric lifetime, often hundreds of thousands of years, and so emissions build up over time, whereas methane, for example, has a shorter atmospheric half-life of about 10 years. This atmospheric lifetime discrepancy leads to the accumulation of CO_2 in the atmosphere, and warming effect, whereas SLCPs do not accumulate, leading to different projected long-term warming effects, to which GWP is insensitive [26]. Moreover, GWP is defined in terms of a single emissions pulse, and so does not necessarily represent the long-term climate effects of emissions *streams*. Pierrehumbert et al. in 2014 [25] argued that "emission metrics that aggregate short-lived and long-lived gases seek to do the impossible." They go on to explain that GWP is insensitive to how GHGs warm the earth, and will place more importance on the mitigation of SLCPs than they merit, since SLCPs do not contribute to long-term warming once emission streams stop or decrease [25].

Some research has focused on adapting GWP to better represent the climate effects of SLCPs. The GWP* metric was developed by Allen et al. [2] with this very goal. This metric was then used ny Costa et al. [8] to estimate the long-term climate effects of the agriculture industry. Pierrehumbert and Eshel [26] attempted to quantify the climate impact of the cattle industry without using CO_2e or GWP metrics, because of the large amount of shorter lived GHGs released by this industry, primarily methane and nitrous oxide. Instead of using any variation on a global warming equivalent metric, these authors suggested looking directly at each GHGs' contribution to temperature perturbations over time [26].

Performing a metric-free analysis that focuses on long-term global temperature perturbation due to any anthropogenic emissions source requires a climate model. While highly detailed atmosphere/ocean general circulation models (AOGCM), or less complex but still sophisticated Earth models of intermediate-complexity (EMIC), may be employed, much simpler reduced-complexity climate models have also been widely used to explore future climate trajectories under different policies, including the HECTOR model [16], MAGICC model [20], the FAIR model [34], and the BEAM model [15]. These models have the advantage of including essential characteristics of the climate response to emissions, but are fast and simple enough to run that many different scenarios can be quickly explored. In this work, we develop a simple reduced complexity model based largely on the HECTOR [16] and BEAM models [15], and similar to that used by Back et al. [6].

Our goal in this work is to estimate the marginal warming attributable to the US beef cattle system through the year 2500. Since the climate response to future emissions scenarios depends upon the background climate state, we drive our climate model with CO_2, N_2O, and CH_4 emissions under extended versions of the four classical Representative Concentration Pathways (RCPs), RCP2.6, RCP4.5, RCP6, and RCP8.5 [19], from the year 1765 through 2500. This yields a baseline temperature anomaly prediction. We then consider a counterfactual where, starting in the year 2000, all emissions attributable to the US beef industry are subtracted from the base RCP scenario. Comparing the resulting temperature anomaly to the baseline anomaly yields an estimate for the *marginal* temperature impact of the beef system. We perform a similar analysis for each individual gas (CO_2, N_2O, and CH_4). This approach is similar to that employed by Reisinger and Clark [31].

US beef cattle emissions were estimated by developing a model US cattle herd that includes all major lifecycle stages in both the beef and dairy systems, including cow/calf on pasture, stocker cattle, and cattle finished either on grass or a high-grain feedlot diet; the model considers the cattle herd in seven distinct regions. Residence times in each stage, diet components, and total dry matter intake were estimated from the literature [5, 4, 32]. For each stage and region, we estimated direct livestock emissions, namely CH_4 emissions from enteric fermentation and manure management, and N_2O emissions from manure management, in terms of emissions per head per day. Beef farm CO_2 operations from fuel/energy use were estimated based on Rotz et al. [32]. We also estimated upstream emissions associated with feed production: N_2O from fertilizer application, CO_2 from fertilizer production, and CO_2 from field work and other farm operations. Since all background RCP scenarios encode an eventual phase-out of fossil fuels, we impose a phase-out of CO_2 for our beef system emissions based on the phaseout expectations of respective RCPs.

Since grass-fed beef take longer to finish, and convert a larger fraction of feed energy to methane, they have generally been considered to have a greater climate impact than grain-finished beef in terms of CO_2e [24, 17]. However, since methane is a short-lived gas, we also make a special study of comparing the temperature impact of a hypothetical US system that is predominantly grass-finished instead of grain-finished.

Overall, we find that, while the climate impact of the US beef system as measured by GWP/CO_2e is dominated by methane, the longer-term temperature impact is predominantly influenced by nitrous oxide, primarily due to manure management. While we also find that although the grass-finished system is marginally more warming than grain-finishing, the difference is smaller than seen in most other works or from using CO_2e as a metric. Thus, beef (and likely dairy) industry mitigation efforts should consider prioritizing longer-lived nitrous oxide emissions over methane abatement.

2 Methods

2.1 Data Sources

2.1.1 Historical Temperature Data

The HadCRUT4 dataset provides global historical surface temperature anomalies since January 1850 [22]. It combines land-surface air temperature (CRUTEM4) and sea-surface temperature (HadSST3) data on a 5-degree grid. We use lumped global average temperature anomaly data for validation of the climate model, as described in the Results.

2.1.2 RCP Scenarios

We use four extended RCP scenario for our historical and background emissions series, RCP8.5, RCP6, RCP4.5, and RCP2.6 (also referred to as RCP3-PD) [21]. The number represents the change in radiative forcing at 2100, in W m^{-2}, relative to pre-industrial conditions. We use annual fossil and land-use change emissions from CO_2, CH_4, and N_2O, from 1765 through 2500, to drive our climate model.

2.1.3 USDA Cattle Data

We gathered data on cattle populations from USDA QuickStats to validate the population numbers predicted by our model [40]. Cattle populations reported were total milk cows, beef cows, cattle on feed, and total cattle. We imposed milk and beef cow numbers by region based on this data, and then compared our summed cattle population across all stages to the USDA total.

2.2 Climate Model

We develop a reduced-complexity climate model for the atmospheric cycles of CO_2, CH_4, and N_2O, associated radiative forcing, and temperature perturbations based on HECTOR v1.0 [16], the BEAM model [15], and Pierrehumbert [25]. In particular, we use a box model for the carbon cycle that considers the upper and lower ocean, CO_2 buffering chemistry in the upper ocean, and biota divided into living vegetation, detritus, and soil compartments with CO_2 fertilization. Methane and nitrous oxide are emitted from both natural and anthropogenic sources and undergo simple first-order decay in the atmosphere. Radiative forcing is determined using equations from [11], and this in turn drives temperature perturbation modeled using a simple two-compartment model of the ocean [25]. The overall framework of the climate model is summarized in Figure 1.

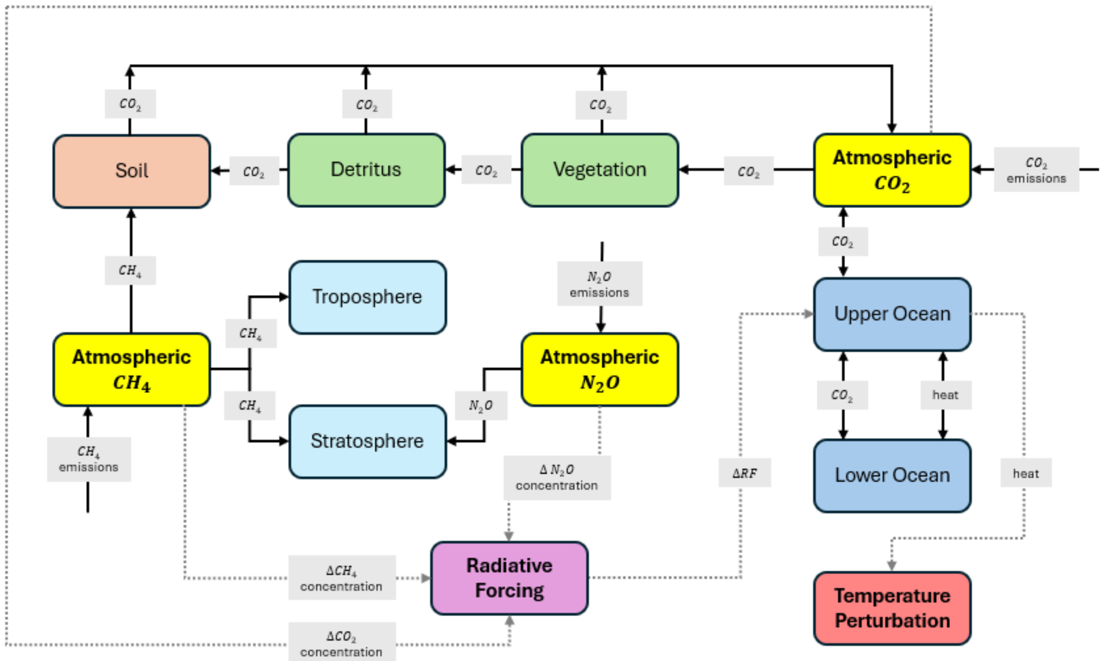

Figure 1: Climate model flowchart

2.3 Carbon Cycle Model

Atmospheric carbon dioxide released into the atmosphere is absorbed by two major sinks: terrestrial biota and the ocean [16]. Terrestrial biota absorb carbon dioxide through photosynthesis; when the plants die and become detritus, the carbon stored in them is then transferred into the soil. During this process, a portion of that carbon is re-released into the atmosphere at each stage. Moreover, the ocean is the largest sink of atmospheric carbon dioxide. Through ocean currents, the carbon absorbed by the surface layer cycles down to the lower ocean. We adopt the overall equation used by Hartin et al. [16] for the change in atmospheric carbon, C_A (moles),

$$\frac{dC_A}{dt} = F_A(t) + F_{LC}(t) + F_O(t) - F_L(t) \tag{1}$$

Where F_A represents fossil and industrial carbon emissions, F_{LC} represents emissions from land-use change, F_O represents atmosphere-ocean flux, and F_L represents the atmosphere-land flux. We perform all calculations using moles as units.

2.3.1 Ocean Carbon Sub-Model

For ocean-atmosphere carbon flux, we adopt the BEAM carbon model presented by Glotter et al. [15], which divides the ocean into upper and lower compartments. There is direct exchange of carbon dioxide between the atmosphere and the upper ocean, which affects pH and carbon buffering chemistry; carbon then cycles down into the lower ocean. The differential equations describing the model follow, with C_A, C_U, and C_L representing the quantities of carbon in the atmosphere, upper ocean, and lower ocean, respectively,

$$\begin{aligned}
F_O(t) &= -k_a C_A + k_a \frac{k_H}{\delta_a \Lambda(t)} C_U, & (2)\\
\frac{dC_U}{dt} &= k_a C_A - k_a \frac{k_H}{\delta_a \Lambda(t)} C_U - k_d Q_U + \frac{k_d}{\delta_d} C_L, & (3)\\
\frac{dC_L}{dt} &= k_d C_U - \frac{k_d}{\delta_d} C_L, & (4)
\end{aligned}$$

where

$$\Lambda(t) = 1 + \frac{K_1}{[H^+]} + \frac{K_1 K_2}{[H^+]^2}, \tag{5}$$

and k_a and k_d (year^{-1}) are time-constants for carbon turnover between the atmosphere and upper ocean, and upper ocean and lower ocean, respectively, δ_d is the ratio of moles of deep ocean to upper ocean, δ_a is the ratio of moles of upper ocean to atmosphere, and $\Lambda = \Lambda(t, [H^+])$ varies with time according to pH, with $[H^+] = [H^+](t)$ the current concentration of hydrogen ions (in mole fraction). The parameters K_1 and K_2 are equilibrium constants for the following series of reactions, whereby CO_2 interacts with water to form bicarbonate and carbonate.

$$\begin{aligned}
CO_2(aq) + H_2O &\rightleftharpoons H_2CO_3, & (6)\\
H_2CO_3 &\rightleftharpoons HCO_3{}^- + H^+, & (7)\\
HCO_3{}^- &\rightleftharpoons CO_3{}^{2-} + H^+. & (8)
\end{aligned}$$

We have total dissolved inorganic carbon as

$$[DIC] = [CO_2(aq)] + [HCO_3{}^-] + [CO_3{}^{2-}], \tag{9}$$

where we lump $CO_2(aq)$ and H_2CO_3 together. Our equilibrium constants for the reactions are, as mentioned above,

$$\begin{aligned}
K_1 &= \frac{[HCO_3{}^-][H^+]}{[CO_2(aq)]}, & (10)\\
K_2 &= \frac{[CO_3{}^{2-}][H^+]}{[HCO_3{}^-]}. & (11)
\end{aligned}$$

We rearrange to get

$$\begin{aligned}
[HCO_3{}^-] &= \frac{K_1[CO_2(aq)]}{[H^+]}, & (12)\\
[CO_3{}^{2-}] &= \frac{K_1 K_2 [CO_2(aq)]}{[H^+]^2}, & (13)
\end{aligned}$$

and plugging into $[DIC]$ gives

$$[DIC] = [CO_2(aq)] \left(1 + \frac{K_1}{[H^+]} + \frac{K_1 K_2}{[H^+]^2}\right). \tag{14}$$

The second term is our $\Lambda(t, [H^+])$, and gives the ratio of total inorganic carbon in the upper ocean to CO_2(aq). This value is uniquely determined by pH, which decreases (i.e., $[H^+]$ increases), over time as carbon is absorbed by the ocean. To calculate $[H^+]$, we approximate the titration alkalinity, Alk, as

$$\begin{aligned}
Alk &= [HCO_3^-] + 2[CO_3^-] = \left(\frac{K_1}{[H^+]} + \frac{2K_1K_2}{[H^+]}\right)[CO_2(aq)] & (15)\\
&= C_U \frac{1}{\Lambda(t)} \left(\frac{K_1}{[H^+]} + \frac{2K_1K_2}{[H^+]}\right).
\end{aligned}$$

Algebra yields

$$[H^+]^2 + [H^+]K_1\left(1 - \frac{C_U}{Alk}\right) + K_1K_2\left(1 - \frac{2C_U}{Alk}\right) = 0, \tag{16}$$

and we take $[H^+]$ as the positive root of this quadratic equation, with Alk taken to be a given constant. Therefore, we can calculate $[H^+]$ from upper ocean ocean carbon content at any time over the course of our simulations.

2.3.2 Biota Carbon Sub-Model

Previous reduced complexity climate models have typically modeled the biota using three compartments, and included loss due to land use change, and increased uptake via CO_2 fertilization. We follow Hartin et al. [16] and use the following system of equations for carbon flux between the atmosphere and living vegetation, C_V, detritus, C_D, and soil, C_S,

$$\frac{dC_V}{dt} = \mathrm{NPP}(t)f_{nv} - C_V(f_{vd} + f_{vs}) - F_{LC}(t)f_{lv}, \tag{17}$$

$$\frac{dC_D}{dt} = \mathrm{NPP}(t)f_{nd} + C_V f_{vd} - C_D f_{ds} - RH_{det} - F_{LC}(t)f_{ld}, \tag{18}$$

$$\frac{dC_S}{dt} = \mathrm{NPP}(t)f_{ns} + C_V f_{vs} + C_D f_{ds} - RH_{soil} - F_{LC}(t)f_{ls}, \tag{19}$$

where NPP is annual net primary productivity (mols C yr^{-1}), f_{nv}, f_{nd}, and f_{ns} give the fractions of NPP allocated to vegetation, detritus, and soil, respectively, f_{vd} and f_{vs} give the fractions of vegetation carbon that transition to detritus and soil each year, respectively, while f_{lv}, f_{ld}, f_{ls} give the fractions of land use change emissions sourced from each biota compartment. Carbon loss to the atmosphere via heterotrophic respiration is given by RH_{det} and RH_{soil}.

Global NPP is assumed to vary with time due to CO_2 fertilization according to Hartin et al. [16], as

$$\mathrm{NPP}(t) = \mathrm{NPP}_0\left(1 + \beta \log\left(\frac{C_A}{C_0}\right)\right), \tag{20}$$

where C_0 is preindustrial atmospheric CO_2 concentration, and β is a scaling parameter. Heterotrophic respiration from detritus and soil, RH_{det} and RH_{soil}, respectively, may increase with temperature as modeled by Hartin et al. [16]. However, we simply assume constant respiration rates, with f_{rd} and f_{rs} the fractions of carbon that oxidize in a year:

$$\mathrm{RH}_{det}(t) = C_D f_{rd}, \tag{21}$$

$$\mathrm{RH}_{soil}(t) = C_S f_{rs}. \tag{22}$$

2.3.3 Parameter values and initial conditions

For the atmosphere-ocean sub-model, we have the following parameter values from [15]: $k_a = 0.2$ yrs^{-1}, $k_d = 0.05$ yrs^{-1}, $\delta_d = 50$, $k_H = 1.23 \times 10^3$ (unitless), $K_1 = 8 \times 10^{-7}$ moles kg^{-1} $= 1.44 \times 10^{-8}$ mole fraction, $K_2 = 4.53 \times 10^{-10}$ moles kg^{-1} $= 8.154 \times 10^{-12}$ mole fraction, and $Alk = 767$ GtC $= 767 \times 10^{15}/12$ moles. We calculate $\delta_a = OM/(AM(1 + \delta_d))$, where $AM = 1.77 \times 10^{20}$ moles (moles in the atmosphere) and $OM = 7.8 \times 10^{22}$ moles (moles in ocean).

Table 1 summarizes the biota-specific parameters and default values.

2.4 Non-CO_2 Gases

2.4.1 Methane Cycle

The major sinks for atmospheric methane emissions are the soil, the stratosphere, and oxidation in the troposphere [16]. During the oxidation process, which is the largest sink, methane reacts with hydroxyl

Parameters	Description	Default Value
NPP_0	Pre-industrial net primary production	50.0 PgC/yr
β	Fractional parameter for carbon fertilization	0.36
f_{ds}	Annual fraction of detritus carbon that is transferred to soil	0.60
f_{ld}	Annual fraction of land use change flux from detritus	0.01
f_{ls}	Annual fraction of land use change flux from soil	0.89
f_{lv}	Annual fraction of land use change from vegetation	0.10
f_{nd}	Annual fraction of NPP carbon that is transferred to detritus	0.60
f_{ns}	Annual fraction of NPP carbon that is transferred to soil	0.05
f_{nv}	Annual fraction of NPP carbon that is transferred to vegetation	0.35
f_{rd}	Annual fraction of respiration carbon that is transferred to detritus	0.25
f_{rs}	Annual fraction of respiration carbon that is transferred to soil	0.02
f_{vd}	Annual fraction of vegetation carbon that is transferred to detritus	0.034
f_{vs}	Annual fraction of vegetation carbon that is transferred to soil	0.001

Table 1: Biota-specific carbon cycle parameters and default values. Adopted partially from Hartin et al. [16].

radicals (HO) present in the air and undergoes a series of reactions that yields carbon dioxide. In the case of biogenic methane, this CO_2 is not new to the short-term carbon cycle, and thus is not counted as a new emission stream to the carbon cycle model. We describe the change in total CH_4 (in moles) in the atmosphere based on the equation used by Hartin et al. [16] as

$$\frac{dCH_4}{dt} = E(CH_4) - \frac{CH_4}{\tau_{OH}} - \frac{CH_4}{\tau_{strat}} - \frac{CH_4}{\tau_{soil}} \tag{23}$$

where $E(CH_4)$ is the total emissions of methane measured in moles yr^{-1}, and τ_{OH}, τ_{strat}, and τ_{soil} give the e-folding times of the tropospheric OH sink, stratospheric sink, and the soil sink, respectively, measured in years.

2.4.2 Nitrous Oxide

The concentration of atmospheric nitrous oxide is dependent on its lifetime, which is approximately 109 years before it, undergoes the photolysis reaction in the stratosphere [28]. We adopt the equation for N_2O in the atmosphere from [16]:

$$\frac{dN_2O}{dt} = E(N_2O) - \frac{N_2O}{\tau_{N_2O}}, \tag{24}$$

where $E(N_2O)$ gives total emissions of nitrous oxide in moles yr^{-1}, N_2O is the present atmospheric level of nitrous oxide (moles), and τ_{N_2O} is the atmospheric lifetime of nitrous oxide measured in years.

2.5 Radiative Forcing

We use the modeled concentration of each GHG in the atmosphere to calculate the associated radiative forcing in W m^{-2}. The values are calculated with the formulae provided by Etminan et al. [11], which account for the overlapping frequencies of electromagnetic radiation absorbed by carbon dioxide, methane, and nitrous oxide, as follows:

$a_1 = -2.4 \times 10^{-7}$ W m^{-2} ppm^{-1}	$b_1 = 7.2 \times 10^{-4}$ W m^{-2} ppm^{-1}	$c_1 = -2.1 \times 10^{-4}$ W m^{-2} ppb^{-1}
$a_2 = -8.0 \times 10^{-6}$ W m^{-2} ppm^{-1}	$b_2 = 4.2 \times 10^{-6}$ W m^{-2} ppb^{-1}	$c_2 = -4.9 \times 10^{-6}$ W m^{-2} ppb^{-1}
$a_3 = -1.3 \times 10^{-6}$ W m^{-2} ppb^{-1}	$b_3 = -8.2 \times 10^{-6}$ W m^{-2} ppb^{-1}	

Table 2: Coefficients for radiative forcing model.

$$RF_{CO_2} = \left[a_1(C - C_O)^2 + b_1|C - C_0| + c_1\bar{N} + 5.36\right] \ln\left(\frac{C}{C_0}\right), \tag{25}$$

$$RF_{N_2O} = \left[a_2\bar{C} + b_2\bar{N} + c_2\bar{M} + 0.117\right] \left(\sqrt{N} = \sqrt{N_0}\right), \tag{26}$$

$$RF_{CH_4} = \left[a_3\bar{M} + b_3\bar{N} + 0.043\right] \left(\sqrt{M} = \sqrt{M_0}\right), \tag{27}$$

with coefficients given in Table 2.

Where C, N, and M are the gas concentrations at the present time; C_0, N_0, and M_0 are the initial pre-industrial concentrations; and $\bar{C}$, $\bar{N}$, $\bar{M}$, are the arithmetic means of the initial and present gas concentrations, e.g., $\bar{C} = 0.5(C_0 + C)$.

Concentrations are measured in parts-per-million by volume (ppm) for CO_2, while concentrations for N_2O and CH_4 are measured in parts-per-billion by volume (ppb). To convert from moles to concentration, we assume an atmosphere with a fixed molar volume, $AM = 1.77 \times 10^{20}$ moles. Taking the sum of RF_{CO_2}, RF_{N_2O}, and RF_{CH_4}, yields an overall time-varying radiative forcing perturbation, which we denote $\Delta N(t)$ in the temperature model below.

2.6 Temperature Model

Imposed emissions streams yield time-varying atmospheric concentrations of our three GHGs, which in turn yield $\Delta N(t)$, the radiative forcing perturbation at any time. We adopt the two-compartment ocean model of Pierrehumbert and Eshel [26] to describe the resulting temperature perturbations in the mixed (upper) and lower ocean, dT'_{mix}, and dT'_{deep}, respectively. Model equations are given as

$$\mu_{mix}\frac{dT'_{mix}}{dt} = -\hat{\lambda}T'_{mix} - \gamma(T'_{mix} - T'_{deep}) + \Delta N(t), \tag{28}$$

$$\mu_{deep}\frac{dT'_{deep}}{dt} = \gamma(T'_{mix} - T'_{deep}), \tag{29}$$

where μ_{mix} and μ_{deep} are the heat capacities of the mixed and deep ocean layers (with $\mu_{deep} \gg \mu_{mix}$), γ is a heat-transfer coefficient for heat transfer from the upper to deep ocean (approximately equal to $\hat{\lambda}$), and $\hat{\lambda} = -\lambda$ is the negation of the climate sensitivity parameter. Pre-industrial initial conditions are $T'_{mix}(0) = T'_{deep}(0) = 0$ K, and we use parameter values from Pierrehumbert and Eshel[26]: $\mu_{mix} = 3.154 \times 10^8$ J m^{-2} K^{-1}, $\mu_{deep} = 6.307 \times 10^9$ J m^{-2} K^{-1}, $\hat{\lambda} = 1.2$ W m^{-2} K^{-1}, and $\gamma = 1.2$ W m^{-2} K^{-1}.

2.7 Global Warming Potential and CO_2-equivalents

In general, GWP for any gas is defined as the ratio of integrated radiative forcing from a one kg pulse emission to some time horizon H, to the integrated radiative forcing due to a one kg CO_2 pulse emission [8]. We adopt the values due to the IPCC Sixth Assessment report of 273 for N_2O and 27 for (non-fossil) CH_4.

2.8 Livestock Model and Marginal Temperature Anomaly

Multiple authors have developed models for the integrated milk and beef herd lifecycles. We propose a differential equations model for this system, which we run to equilibrium to obtain steady-state cattle populations. We determine direct emissions per head (due to enteric fermentation and manure management) for each lifecycle stage, farm and also estimate upstream emissions per head from farm operations and feed production. Given these emissions streams and equilibrium cattle populations, we determine the total emissions attributable to the beef system (we omit beef production from milk cows and dairy culls). Then, the climate model is driven using a baseline RCP scenario with or without these emissions after 2000.

The temperature perturbation at 2500 for each case is compared, allowing us to estimate the marginal temperature effect of the beef herd. Moreover, we perform the same procedure but drive the model with a single gas, allowing us to to determine the marginal warming due to each particular gas. We also calculate total CO_2e for the beef emissions stream, through 2500.

Finally, since CO_2 from fossil emissions is, in the long-term, phased out to zero under all RCP scenarios, we also impose a CO_2 phase-out schedule for our beef herd emissions. We impose a linear phase-out over the years 2020 through 2100 for RCP2.6, 2050 through 2150 for RCP4.5, 2080 through 2150 for RCP6, and 2100 through 2250 for RCP8.5.

2.8.1 Cattle Herd Model

Our beef model represents typical U.S. beef production practices, breaking the life cycle into three stages: cow/calf, stocker or backgrounding, and finishing. Each stage has regional nuances and different emission contributions. Based on Rotz et. al [32] and several papers by Asem-Hiablie and colleagues [5, 4] we determined reasonable values for the rates driving our model and summarized below.

We impose milk and beef cow populations by allocating calf fluxes to the replacement heifer compartments such that, at equilibrium, the desired cow population is obtained (these populations are set based on USDA data).

Parameter	**Value**	**Description (all rates are in 1/year)**
M_b	0.9000	rate of milk cows giving birth
M_m	0.5000	rate of dairy heifers becoming dairy cows
M_f	1.0000	rate of dairy feedlot being culled
M_p	0.3300	rate of dairy cows being culled
B_b	0.9000	rate of beef cows giving birth
B_m	0.5000	rate of beef heifers becoming beef cows
B_{f2f}	0.5000	rate of hay-forage feedlot going to grain-finish stage
ghf	0.3904	rate of stocker going to grain-finish stage
gsf	0.0411	rate of stocker going to grass-finish stage
gsp	1.0000	rate of grass-finish lot going to production
ghp	1.0000	rate of grain-finish lot going to production
B_p	0.1500	rate of beef cows being culled

Table 3: Table of cow population dynamical model parameters with values and descriptions.

The differential equations model follows as,

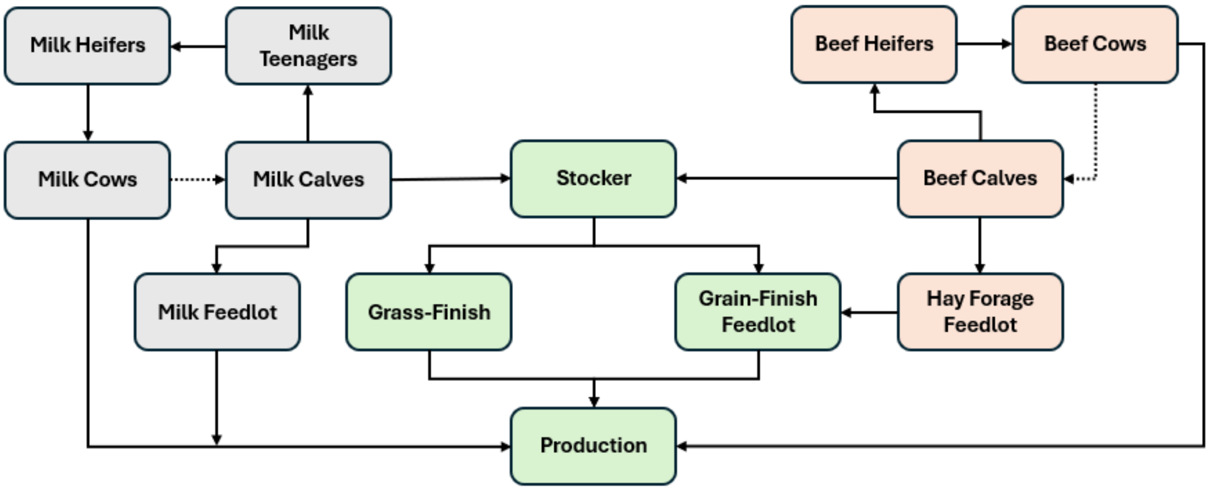

Figure 2: Dairy and beef lifecycle model flowchart.

$$M_h = \text{rate\_}M \cdot \min\left(\frac{1}{2}, \frac{M_p \cdot \text{milk\_cattle\_val}}{M\text{\_calves} \cdot 2}\right) \tag{30}$$

$$M_s = \text{rate\_}M \cdot \frac{1}{3} \cdot (1 - M_h) \tag{31}$$

$$M_{cf} = \text{rate\_}M \cdot \frac{2}{3} \cdot (1 - M_h) \tag{32}$$

$$B_h = \text{rate\_}B \cdot \min\left(\frac{1}{2}, \frac{B_p \cdot \text{beef\_cattle\_val}}{B\text{\_calves} \cdot 2}\right) \tag{33}$$

$$B_s = \text{rate\_}B \cdot 0.99 \cdot (1 - B_h) \tag{34}$$

$$B_f = \text{rate\_}B \cdot 0.01 \cdot (1 - B_h) \tag{35}$$

$$\frac{dM\text{\_cows}}{dt} = M_m \cdot M\text{\_heifers} - M_p \cdot M\text{\_cows} \tag{36}$$

$$\frac{dM\text{\_calves}}{dt} = M_b \cdot M\text{\_cows} - M_h \cdot M\text{\_calves} - M_s \cdot M\text{\_calves} - M_{cf} \cdot M\text{\_calves} \tag{37}$$

$$\frac{dM\text{\_heifers}}{dt} = M_h \cdot M\text{\_calves} - M_m \cdot M\text{\_heifers} \tag{38}$$

$$\frac{dM\text{\_feedlot}}{dt} = M_{cf} \cdot M\text{\_calves} - M_f \cdot M\text{\_feedlot} \tag{39}$$

$$\frac{dB\text{\_heifers}}{dt} = B_h \cdot B\text{\_calves} - B_m \cdot B\text{\_heifers} \tag{40}$$

$$\frac{dB\text{\_cows}}{dt} = B_m \cdot B\text{\_heifers} - B_p \cdot B\text{\_cows} \tag{41}$$

$$\frac{dB\text{\_calves}}{dt} = B_b \cdot B\text{\_cows} - (B_h + B_f + B_s) \cdot B\text{\_calves} \tag{42}$$

$$\frac{dB\text{\_hff}}{dt} = B_f \cdot B\text{\_calves} - B_{f2f} \cdot B\text{\_hff} \tag{43}$$

$$\frac{d\text{stocker}}{dt} = M_s \cdot M\text{\_calves} + B_s \cdot B\text{\_calves} - (\text{ghf} + \text{gsf}) \cdot \text{stocker} \tag{44}$$

$$\frac{d\text{GrassFinish}}{dt} = \text{gsf} \cdot \text{stocker} - \text{gsp} \cdot \text{GrassFinish} \tag{45}$$

$$\frac{d\text{GrainFinish}}{dt} = \text{ghf} \cdot \text{stocker} - \text{ghp} \cdot \text{GrainFinish} \tag{46}$$

$$\frac{d\text{production}}{dt} = M_p \cdot M\text{\_cows} + \text{gsp} \cdot \text{GrassFinish} + \text{ghp} \cdot \text{GrainFinish} + B_p \cdot B\text{\_cows} + M_f \cdot M\text{\_feedlot} \tag{47}$$

Model variables follow:

- M_h: Represents the rate of change at which milk calves become heifers, taking into account the rate of milk cattle and a limiting factor based on the population of milk calves.
- M_s: Represents the rate at which milk calves move to the stocker stage.
- M_{cf}: Represents the rate of change at which milk calves move to the feedlot.
- B_h: Represents the rate of change at which beef calves become heifers, with a limiting factor based on the population of beef calves.
- B_s: Represents the rate of change at which beef calves move to the stocker stage.
- B_f: Represents the rate of change at which beef calves move to the feedlot.
- M_cows: The number of milk cows.
- M_calves: The number of milk calves.
- M_heifers: The number of milk heifers.
- M_feedlot: The number of animals in the feedlot.
- B_heifers: The number of beef heifers.
- B_cows: The number of beef cows.
- B_calves: The number of beef calves.
- B_hff: The number of beef cattle in hay-forage feedlot.
- stocker: The number of stocker cattle.
- GrassFinish: The cattle in grass finishing stage.
- GrainFinish: The cattle in grain finishing stage.
- production: The overall number of cattle sent to production, including all transitions leading to slaughter.

2.9 Cattle-Associated Emissions

We determine direct livestock emissions from estimated dry matter intake (DMI) and feed type at each production stage, which yields methane from enteric fermentation and manure, and nitrous oxide from manure management. Carbon dioxide emissions from on-farm operations are also included in direct emissions.

Indirect emissions include those attributable to beef farm/ranching operations, and the upstream emissions embodied in feed production. With respect to the latter, we consider N_2O from nitrogen fertilizer application, CO_2 from fertilizer production, and CO_2 from upstream farm and field operations.

Emissions of each gas were calculated in kg of GHG per cow, per year, for each stage and for each region. Our cattle emission stages are cow/calf, stocker, backgrounding (i.e., forage-heavy grower diet in feedlot), grain-finish feedlot, and grass-finishing. Replacement heifers are lumped into the cow/calf stage, with each heifer weighted as 2/3 of a cow/calf pair; Calf populations are not explicitly considered.

2.9.1 Direct Emissions

Direct emissions from cattle farming are CH_4 released from enteric fermentation and manure, N_2O released from manure, and CO_2 released from farm operations.

For forage-based feeds, like grass grazed on pasture, hay, and silage, roughly $6.5\% \pm 1$ of gross energy (GE) of feed consumed is converted into CH_4 via enteric fermentation. For grain-based feed, primarily used at the feedlot stage, about $3\% \pm 1$ GE of feed consumed is converted into CH_4 [9].

Our enteric fermentation CH_4 emission formula is taken directly from Gibbs [14]:

$$\text{Enteric CH}_4 \text{ Emissions (kg/yr)} = [\text{Intake(MJ/day)} \cdot \text{Y}_m \cdot \text{(365 days/yr)}]/[\text{55.65 MJ/kg of methane}] \quad (48)$$

Enteric CH_4 is the amount of CH_4 released from enteric fermentation of feed in kg/cow/yr. Intake refers to the gross energy intake of feed by one cattle in MJ/day. Y_m is the methane conversion rate, or the percentage of gross energy intake of feed which becomes CH_4. Energy intake is determined from DMI and feed energy content. We assume DMI is roughly 10kg at each stage, based on [32], and feed breakdowns follow: In the cow/calf stage cows are primarily grazing on pasture while consuming a small amount of supplementary hay. We estimated intake is 2/3 pasture to 1/3 hay at the cow/calf stage. We assumed a similar diet for stocker cattle. If cattle are backgrounded, we assume a diet consisting of 75% hay silage or haylage and 25% corn silage. Gross energy stored in pasture is estimated at approximately 18.3 MJ/kg DM while cut pasture or hay has an estimated gross energy of approximately 18 MJ/kg DM [5] [1].

Total energy intake is calculated with the following formula:

$$\text{Intake (MJ/day)} = \sum_i (\text{F}_i \cdot \text{GE}_i \cdot \text{DMI}) \quad (49)$$

Associated methane emissions are then calculated as:

$$\text{Intake (MJ/day)} \cdot \text{Y}_m = \sum_i (\text{F}_i \cdot \text{GE}_i \cdot \text{DMI} \cdot \text{Y}_{mi}), \quad (50)$$

where F_i is the percentage of feed i in the diet, GE_i is the gross energy in MJ per kilogram of dry matter for feed i, and DMI is dry matter intake. Y_{mi} is the percentage of gross energy intake of feed i which becomes CH_4.

Methane emissions from cattle manure are given by Gibbs, Jun, and Gaffney [13]:

$$\text{EF}_{CH_4-manure} = \text{VS}_i \cdot \text{365 days/yr} \cdot \text{B}_{oi} \cdot 0.67\text{kg/m}^3 \cdot \sum_{jk} \text{MCF}_i \cdot \text{MS\%}_{ijk} \quad (51)$$

$EF_{CH_4-manure}$ is the annual emission factor for CH_4 from cattle manure in kilograms per cow per year, VS is the daily volatile solid excreted in kilograms, and B_o is the maximum methane production capacity (m^3/kg of VS) for manure produced. This varies between dairy and beef cattle, but since we only consider emissions from beef cattle, B_o is kept constant across all cattle stages. The parameter MCF_i represents the methane conversion factor for region i, which varies based on manure management system of the cattle stage, and temperature of region i, and $MS\%_{jk}$ is the fraction of manure handling system using manure system j in climate region k. In this work, each cattle lifecycle stage was assumed to use 100% of one type of manure storage system, so $MS\%_{jk}$ was always set to 1. See Table 5 for the values of these parameters. We multiply by 365 to convert to emissions per year, and we multiply by 0.67 to convert from m^3 of methane to kilograms of methane.

The formula for VS_i is also given by Gibbs, Jun, and Gaffney [13]:

$$\text{VS}_i = \mathit{Intake} \cdot (\text{1 kg DM/18.45MJ}) \cdot (1 - \text{DE}/100) \cdot (1 - \text{ASH}/100) \quad (52)$$

Intake in MJ/day is calculated as above, DE is the percentage of feed i that is digestible energy, and ASH is the percentage of feed i that is ash.

The formula for N_2O released from manure is:

$$\text{Manure } N_2O = \text{DMI} \times \text{CP} \times \text{CP}_{excreted} \times \text{EF}_m \times (365 \times 44/28)/6.25 \tag{53}$$

DMI is the dry matter intake at a given cattle stage, $CP_{excreted}$ is the percentage of CP consumed that is excreted, and EF is the emission factor of N_2O released from manure in management system m, which was kept constant at 0.2.

Table 4: **Feed characteristics**

Feed Type	**Gross Energy (MJ)**	**Digestible Energy (%)**	**Ash content (%)**	**Crude Protein (%)**
Pasture [42] [a]	18	55.8	9.5	10
Hay/Haylage	18.1 [37]	55.8	9.5	14 [39]
Corn grain	21	83	6	10
Corn Silage	19	60	5	8.5 [29]

Table 5: **Direct Emission Parameters**

Parameter	**Unit**	Beef Cow	Heifer	Stocker	Background	Grain-finish feedlot	Grass-Finish
DMI	**kg/day**	10.269	6.846	10	10	10	10
B_o [13]	m^3/kg	0.17	0.17	0.17	0.17	0.17	0.17
$CP_{excreted}$	%	93	93	93	85	80	93
MCF_{SW}	%	1.5	1.5	1.5	1.5	1.5	1.5
MCF_{NW}	%	1.0	1.0	1.0	1.0	1.0	1.5
MCF_{MW}	%	2.0	2.0	2.0	5.0	5.0	1.5
MCF_{SP}	%	1.0	1.0	1.0	1.0	1.0	1.5
MCF_{NP}	%	1.5	1.5	1.5	1.5	1.5	1.5
MCF_{SE}	%	2.0	2.0	2.0	5.0	5.0	1.5
MCF_{NE}	%	1.5	1.5	1.5	1.5	1.5	1.5

We derived CO_2 emissions from beef farm operations directly from estimations provided by Rotz et al. [32] which provided CO_2 emissions in grams per kg carcass weight. We converted these to emissions per head for each herd stage based on modeled population sizes for each region.

2.9.2 Upstream Emissions

Emissions from feed production include CO_2 emissions from farm operations and the feed production process, as well as N_2O emissions from the application of nitrogen-based fertilizer to feed crops. For our research, we made the assumption that all nitrogen-based fertilizer used was urea, since that is the dominant type of nitrogen fertilizer [22]. Emissions from urea fertilizer application to feed are calculated using:

$$EF_{N_2O-fert} = \frac{\text{fert}_{Nj}}{\text{yield}_j} \times \frac{1}{\text{DM}_j} \times \text{EF}_{N-N_2O} \times \frac{44}{28} \times \%\text{ff}_j \times \text{DMI}_k \times \text{bd}_k \times 365 \tag{54}$$

$\text{EF}_{N_2O-fert}$ is the N_2O emission in kilograms per cow per year from the application of nitrogen based fertilizer to feed, fert_{Nj} is the amount of N applied per acre of feed j, yield_j is the yield of feed j per acre,

Parameter	Unit	Value
FPC_N	kg	3.1 [36]
$FPC_{P_2O_5}$	kg	1.0 [36]
FPC_{K_2O}	kg	0.7 [36]
$fert_{Nc}$	kg	67.6 [41]
$fert_{Pc}$	kg	31.3 [41]
$fert_{Kc}$	kg	39.5 [41]
$fert_{Nh}$	kg	18.1 [12]
$yield_{cg}$	kg	3991.6 [40]
$yield_{cs}$	kg	18234.4 [40]
$yield_h$	kg	2068.4 [3]
DM_{cg}	%	85
DM_{cs}	%	32.5 [7]
DM_h	%	90 [30]
I_{N-c}	%	98 [41]
$I_{P_2O_5-c}$	%	79 [41]
I_{K_2O-c}	%	63 [41]
I_{N-h}	%	100
EF_{N-N_2O}	%	1.25 [35]

Table 6: Upstream Emission Parameters

EF_{N-N_2O} is the percentage of N applied that becomes N_2O, %ff is the percent of feed j that is fertilized with Urea fertilizer, DMI_k is the dry matter intake of cattle at emission stage k, and bd_k is the percent of feed k that is in the diet at the observed cattle stage. See Table 6 for parameter values.

For fertilizer production, we considered the CO_2 emissions. We deemed N_2O and CH_4 emissions from fertilizer production negligible [36]. Corn grain and corn silage were also assumed to have the same emissions factor from fertilizer production, and so are generally referred to as corn in Tables 8 and 10 .

$$EF_{CO_2-fert} = FPC_i \times \frac{fert_{ij}}{yield_j} \times \frac{1}{DM_j} \times DMI_k \times I_{i-j} \tag{55}$$

EF_{CO_2-fert} is the CO_2 emission in kilograms per cow per year, from fertilizer production of urea, phosphate, and potash fertilizers; FPC_i is the CO_2 produced per kilogram of nutrient i from the production and transportation of fertilizer; $fert_{ij}$ is the amount of nutrient i applied per acre of feed j; $yield_j$ is the yield of feed j per acre; is the DM_j % of feed j that is dry matter; DMI_k is the dry matter intake of cattle at emission stage k; I_{i-j} is the % of feed j fertilized with nutrient i in the US. See Table 6 for parameter values.

CO_2 from feed production, aside from those associated with fertilizer, came from field work, irrigation, and corn grain drying. These emissions were calculated by summing up the CO_2 emissions in kg per acre associated with each of these emission sources, and then converting to kg CO_2 per kg DM with the known yield per acre of different feeds. We found 0.7 kg CO_2 released per kg DM for corn grain, 1.3 kg CO_2 released per kg DM for corn silage, and 0.6 kg CO_2 released per kg DM for hay/haylage. Through the known DMI at each cattle stage, these emission factors were then converted into kg CO_2 per cow.

3 Results

3.1 Climate Model Under Historical and RCP Emissions

3.1.1 Historical and Model Predictions

Figure 3 compares historical temperature records, a LOESS smoothing function, and model predictions from 1850 to 2000, demonstrating that the model captures historical trends well. The RMSE and MAE for the model compared to historical data are 0.061 and 0.048, respectively. Our model decently captures the trend of the LOESS average.

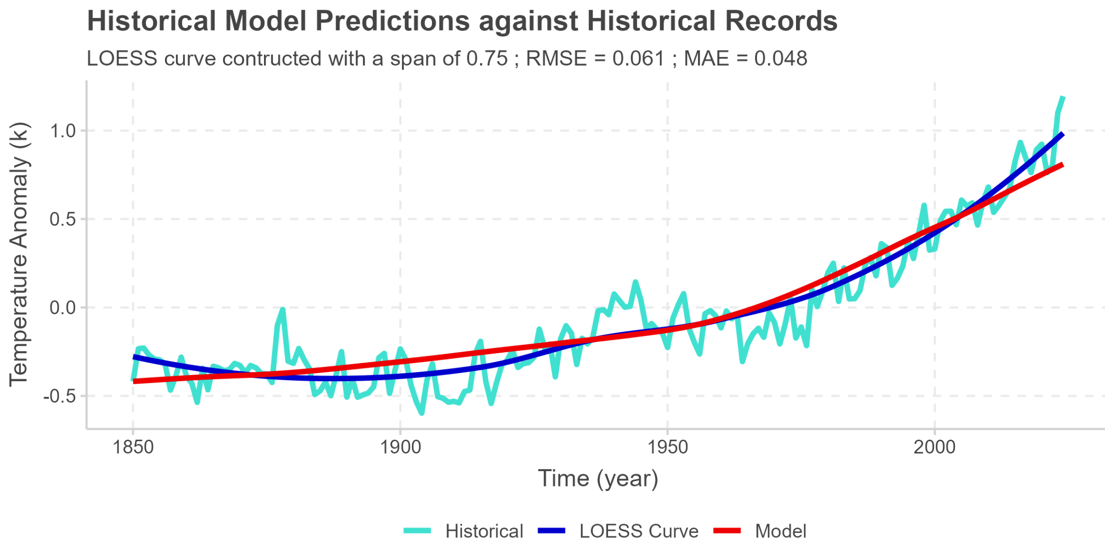

Figure 3: Predicted temperature change from model against historical data

3.1.2 Model Predictions to 2500 Under RCP Scenarios

We also utilized the model to compare the temperature perturbations based on the concentration of the greenhouse gases according to each RCP scenario. We ran our climate model using CO_2, CH_4, and N_2O emissions for each RCP scenario, as shown in Figure 4. The temperature change for RCP 4.5 and 6 is around 2.6 K and 4.8 K respectively, but for the extreme RCP 8.5, this temperature change goes above 7.7 K.

3.2 Modeled Regional Cattle Herd

Using ODE methods, the differential equations model describing cattle dynamics were solved to equilibrium to yield constant cattle populations. The results are shown in Figure 5. Overall, the milk cow population showed varying trends across regions, with the midwest and southern plains having the highest populations, and beef cow populations were highest in the midwest and southern plains as well. Stockers and feedlot cattle were similarly high in the two regions.

To validate the results obtained from the cow herd differential model, we compared the model's output with USDA data; USDA data is presented in Figure 6. The comparison indicates that the differential model is able to calculate the total cow populations, including calves, with relatively small margins of error when compared to the USDA data. We note good concordance between the model predictions and the USDA data particularly in the southern plains and northern plains regions.

3.3 Bottom-Up Beef Emissions

Here we summarize emissions by beef system stage and source, and provide more detailed results for the southwest region (see Tables 9, 8, and 10). Enteric fermentation represented the largest CH_4 emission stream of the cattle system. The greatest amount of CH_4 per cow released was from the beef cow/calf system, and by far the lowest was at the grain-finishing stage, due to the higher digestible energy content of the grain-finishing diet. Depending on the manure management system employed and the climate of the region, manure produces varying amounts of both CH_4 and N_2O, and these emissions are summarized in

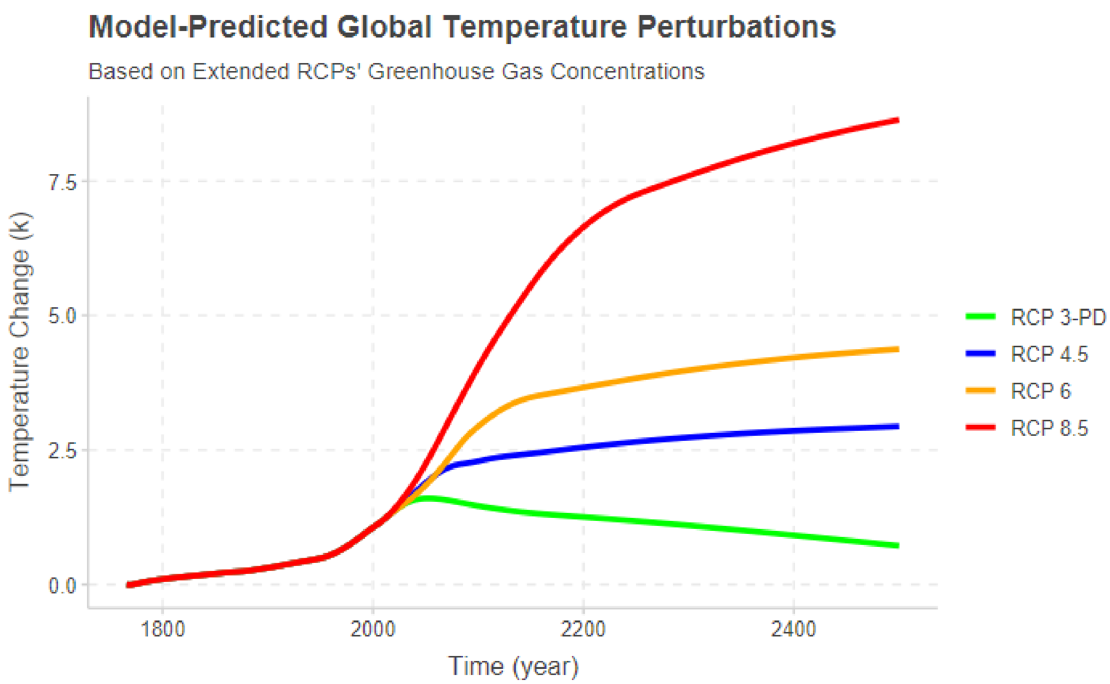

Figure 4: Predicted temperature change from model using different RCP scenarios

Table 9. Manure represented the largest emission source for N_2O, beating out N fertilizer application. Within manure N_2O emissions, the beef cow/calf stage was responsible for the highest proportion of emissions, and the backgrounding stage was the lowest emitter. These results are shown in Tables 9 and 10.

Fuel, electricity, and natural gas used for farm operation all yield CO_2 emissions. Table 9 also summarizes these emissions. For CO_2 attributable to feed production, emissions from hay/haylage were greatest in total, as hay is used for all cattle stages cattle stages, whereas we included corn grain in the cattle diet only for the grain finishing stage, and only the background and grain finishing stage used corn silage. Within hay/haylage emissions, the background stage released the highest CO_2 emissions, with 1512.8 kg per cow in the southwest. CO_2 released from corn grain production was the second highest overall, followed by corn silage production (Table 8).

The fertilization of corn grain with N fertilizer represents the highest upstream emissions source of N_2O in the southwest region due to feed fertilization, both per cow (1 kg/cow/yr 8), and overall (1325409 kg/yr; Table 10), even with corn grain only being used at the finishing stage. This is followed by N fertilizer applied to hay/haylage, and lastly N fertilizer applied to corn silage. For CO_2 emissions from fertilizer production, we found that most was released in the southwest from the production of N-based Urea fertilizer, used both on corn and hay/haylage (Table 10).

3.4 Gas-specific Emissions by Region

Figures 7-9 give total gas-specific emissions for each region. In general, total emissions from the southern plains region are highest across gases, although CO_2 are somewhat disproportionally higher in the midwest.

3.5 Future Warming Attributable to Model Beef System

The total temperature perturbation that can be credited to beef industry emissions is shown in Figure 10, using RCP4.5 for baseline emissions. At the year 2500, the temperature change from the emissions of all 3

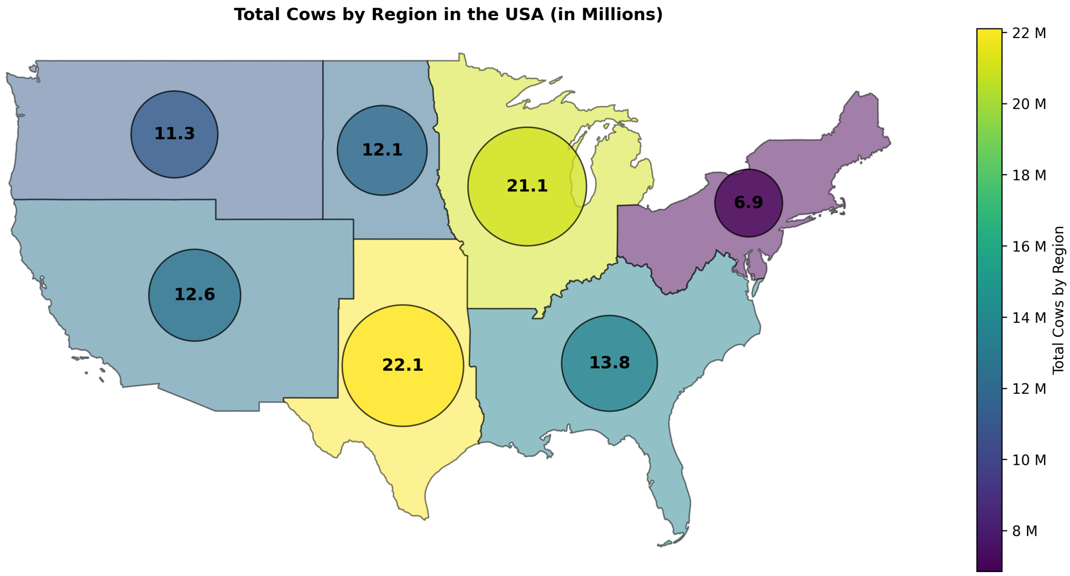

Figure 5: Total Cows by Region in the USA as per our Dynamical Cow Population Model (in Millions).

Table 7: Direct Livestock and Farm Emissions in kg/cow/yr in the SW

Emission-Source	Cattle Stage	Emissions (kg/cow/yr)
Enteric CH_4	Beef Cow	79.2
	Stocker	77.2
	Background	67.9
	Grain-finish	46.2
	Grass-finish	77.0
Manure CH_4	Cow/Calf	2.5
	Stocker	2.4
	Background	2.5
	Grain-finish	1.6
	Grass-finish	2.4
Manure N_2O	Cow/Calf	2.0
	Stocker	1.9
	Background	2.0
	Grain-finish	1.5
	Grass-finish	1.8
Farm Operations CO_2	Cow/Calf	163.0 kg
	Stocker	350.0 kg
	Background	30.2 kg
	Grain-finish	30.2 kg
	Grass-finish	350.0 kg

Table 8: Upstream Emissions in kg/cow/yr in the SW

Emission-Source	Cattle Stage	Emissions (kg/cow/yr)
N2O - N fertilizer application to corn grain	Grain finish	1.0
N2O - N fertilizer application to corn silage	Background	0.2
	Grain-finish	0.1
N2O - N fertilizer application to hay/haylage	Beef Cow/Calf	0.2
	Stocker	0.2
	Background	0.5
	Grain-finish	0.1
	Grass-finish	0.1
CO2 - N fertilizer used on corn production	Background	22.8
	Grain-finish	77.6
CO2 - P fertilizer used on corn production	Background	6.6
	Grain-finish	22.6
CO2 - K fertilizer used on corn production	Background	4.7
	Grain-finish	15.9
CO2 - N fertilizer used on hay/haylage production	Beef Cow/Calf	37.7
	Stocker	36.8
	Background	82.7
	Grain-finish	16.5
	Grass-finish	22.0
CO2 - hay/haylage production	Beef Cow/Calf	690.5
	Stocker	672.4
	Background	1512.8
	Grain-finish	302.6
	Grass-finish	403.4
CO2 - corn grain production	Grain finish	939.5
CO2 - corn silage production	Background	600.8
	Grain-finish	360.5

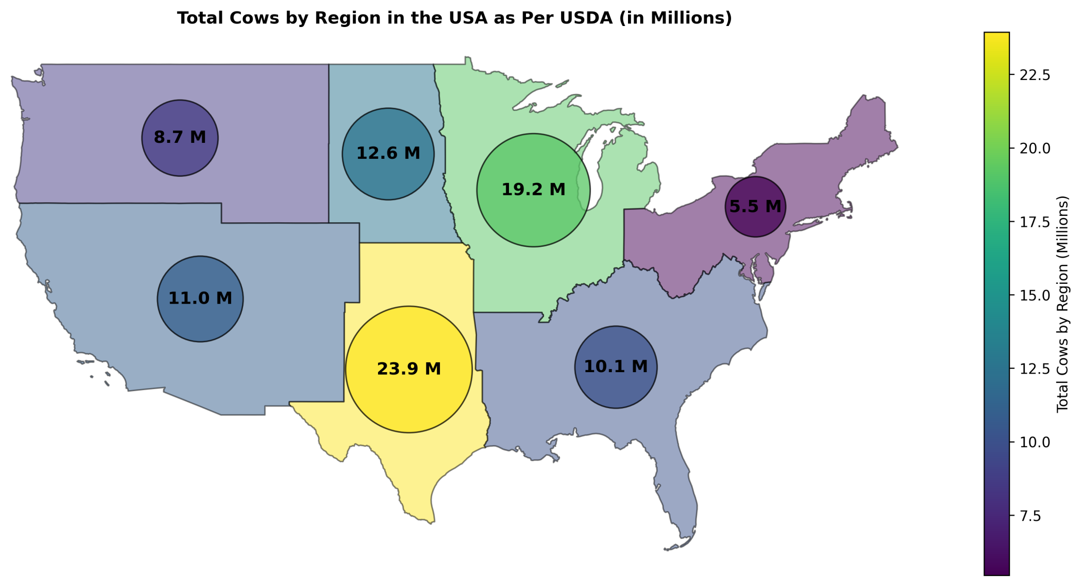

Figure 6: Total Cows by Region in the USA as per USDA (in Millions).

greenhouse gases amount to a global temperature change of 0.0125 Kelvin.

3.5.1 Warming by Gas

Figure 10 shows the total temperature perturbation credited to beef industry emissions disaggregated into the respective contributions by the major greenhouse gases. Among the three, N_2O is revealed to be the predominant driver of temperature perturbation, with roughly 69.7% of the change being caused by nitrous oxide emissions.

3.5.2 Warming Attributable to Each Region

Each U.S. region's role in contributing to the model's projected global temperature perturbation is shown in Figure 12. The map highlights the southern plains as the region with the most emissions, and the midwest as the region with the second most emissions.

3.6 Grain vs. Grass-Finished System

Finishing on a grain-based diet is standard in the United States' beef industry. Compared to grass-finishing, when cattle are finished on a grain-based diet they remain in the system for shorter periods of time, which reduces all direct cattle emissions. They also produce less methane due to enteric fermentation. We explored what the climate impact of the industry would be if cattle were instead primarily finished on a grass-based system. A comparison of the temperature perturbations as a result of the current/grain-finished scenario and a scenario where most cattle are grass-finished are illustrated in Figure 14. It is shown that regardless of the background emissions from other industries, the grass-fed scenario always results in marginally larger temperature changes. In both scenarios, much of the warming can be attributed to N_2O emissions. The temperature changes credited to N_2O often increase with the change to a grass-fed finishing system, with an exception in the RCP 4.5 case. The switch from grain-finishing to grass-finishing also consistently result in a small increase in the temperature attributable to CH_4. However, depending on the background emissions, total temperature perturbations attributable to CO_2 can either increase or decrease.

Table 9: Total GHG emissions from livestock and farm operations, in the SW, in kg/yr

Compound	Cow-Stage	Emissions (kg/yr)
Enteric CH_4	Beef Cow/Calf	192514890
	Stocker	75818349
	Background	1094234
	Grain-finish	62548289
	Grass-finish	5522508
Manure CH_4	Beef Cow/Calf	6105280
	Stocker	2404449
	Background	40950
	Grain-finish	2131252
	Grass-finish	175137
Manure N_2O	Beef Cow/Calf	4826394
	Stocker	1900784
	Background	32012
	Grain-finish	2072835
	Grass-finish	132227
Farm Operations CO_2	Beef Cow/Calf	396008172
	Stocker	343892527
	Background	486975
	Grain-finish	40855617
	Grass-finish	25104154

With the total emissions of each greenhouse gas from the cattle herd model, we also quantified the global climate impact of the emissions in terms of kg CO_2 equivalents in order to evaluate the metric against our temperature perturbation model. The results are shown in Figure 15, and it echoes the results of our model in regards to the small increase in total temperature perturbation when switching to a primarily grass-based finishing system. However, the CO_2e results differs greatly from the results of our model in the amount of climate impact attributed to each GHG. In both cattle-finishing scenarios, the CO_2e results credited CH_4 as the largest contributor of global warming, in contrast to our model which deemed N_2O as the largest contributor. This could be due to the use of GWP-100 in calculating the CO_2e for non-CO_2 gases, which can potentially lead to misleading results for different time scales.

4 Discussion

We have estimated the marginal long-term warming impact of the US beef system using a reduced-complexity climate model coupled to a regional beef-herd model, finding that the long-term temperature impact is likely dominated by N_2O emissions stemming from manure management primarily, and secondarily from feed production. This conclusion is at odds with that implied by the CO_2e and GWP metrics: GWP predicts that methane has the greatest warming effect, in sharp contrast to our results. This suggests a failure of the GWP metric when looking at the long-term warming effects of SLCPs in general, and the beef industry in particular. This result supports the notion that GWP misrepresents the effects of CH_4 and N_2O, as predicted by many other authors [25, 18, 31].

The strong warming effect of N_2O is related to our long timescale and the gas' relatively long atmospheric e-folding time of $\tilde{1}10$ years. Unlike CH_4, N_2O seems to only start to reach a steady state, in terms of warming, at 2500. Since N_2O is sourced from urea fertilizer application and cattle manure in our model, efforts towards reducing the N_2O emissions from these sources should be a focus of mitigation efforts.

The large majority of our total methane emissions come from the cow/calf stage, which can be seen in our representative southwest region in Table 9. This is due to the majority of cattle existing at this stage

Table 10: Total GHG emissions from upstream feed and fertilizer production, in the SW, in kg/yr

Emission-Source	Cattle Stage	Emissions (kg/cow/yr)
N2O - N fertilizer application to corn grain	Grain finish	1325409
N2O - N fertilizer application to corn silage	Background	3230
	Grain-finish	162605
N2O - N fertilizer application to hay/haylage	Beef Cow/Calf	565908
	Stocker	228867
	Background	8451
	Grain-finish	141803
	Grass-finish	10024
CO2 - N fertilizer used on corn production	Background	368128
	Grain-finish	105008269
CO2 - P fertilizer used on corn production	Background	107227.82547604789
	Grain-finish	30586648
CO2 - K fertilizer used on corn production	Background	75472.44042928288
	Grain-finish	21528451
CO2 - N fertilizer used on hay/haylage production	Beef Cow/Calf	91712981
	Stocker	36119423
	Background	1333730
	Grain-finish	22379143
	Grass-finish	1582031
CO2 - Hay/haylage production	Beef Cow/Calf	1677467309
	Stocker	660638777
	Background	24394462
	Grain-finish	409323528
	Grass-finish	28935978
CO2 - corn grain production	Grain-finish	1270958548
CO2 - corn silage production	Background	9688541
	Grain-finish	487702651

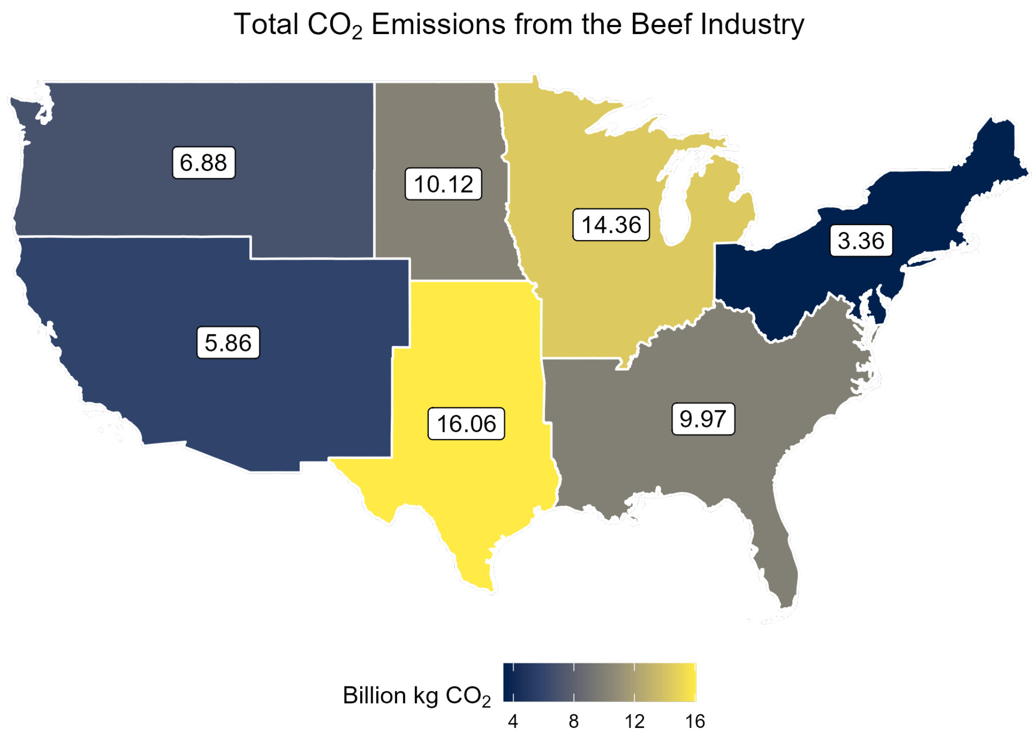

Figure 7: Predicted total CO_2 emissions for the beef cattle industry

in the lifecycle. Rotz et al. [32] supports this, with most of their estimated methane emissions due to the cow/calf stage, and a smaller proportion due to stocker and finishing stages. We found that N_2O emissions also mainly came from the cow/calf stage, which was also found in the Rotz et al. beef industry emission analysis [32]. However, whereas we found the finishing stages to produce slightly more CO_2 than the cow/calf stage, Rotz et al. found the reverse. This is likely due the fact that in our study, we have many emission streams from CO_2, especially for the finishing stages, from the production and fertilization of feed, whereas many of these emission streams don't exist for the cow/calf stage, due to cattle mostly grazing on pasture.

The southern plains region (Texas, Oklahoma, and Kansas) was found to produce the most emissions across all three greenhouse gases, and have the most associated long-term warming. This was an expected result: Rotz et al. [32] also found the most emissions of each GHG in the southern plains through their analysis of the emissions of the US beef industry. This is mainly due to the region hosting more beef industry cattle than any other region.

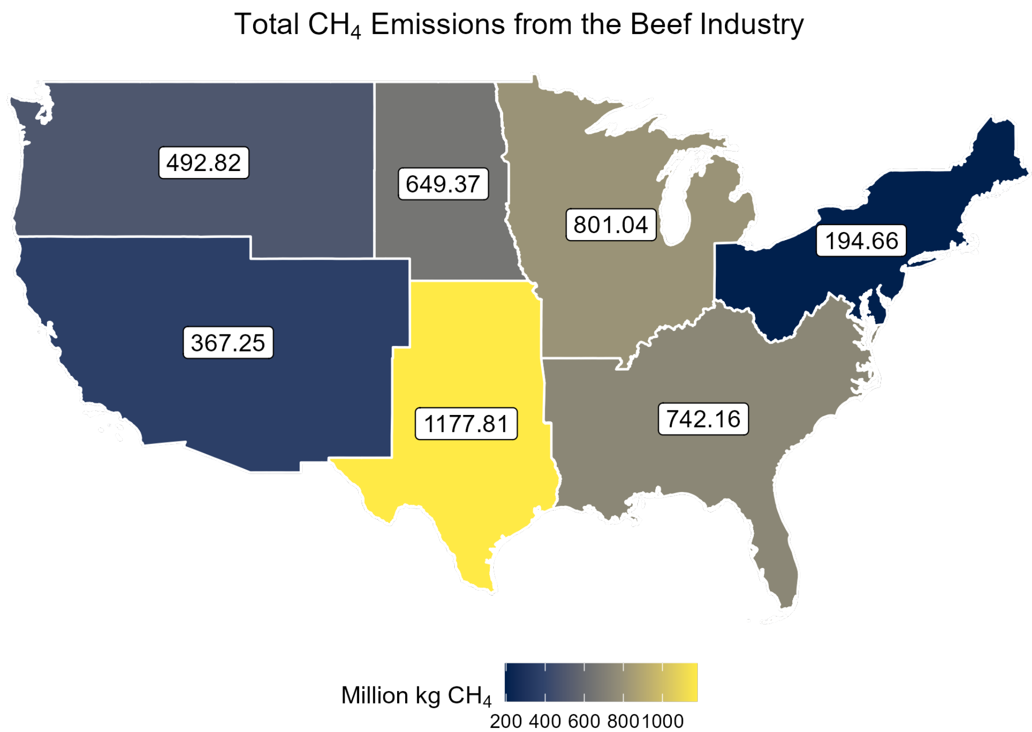

Figure 8: Predicted total CH_4 emissions for the beef cattle industry

When considering cattle finished on pasture (grass-finished) versus cattle finished on grain in feedlots, increased grass-finishing was found to lead to slightly greater long-term warming for all RCP scenarios. This result is supported by Pierrehumbert and Eshel [26], which looked into the emissions and long-term warming from different grass-fed and grain-fed cattle systems. Grass-fed systems release more enteric CH_4, but are associated with lower emissions from farm equipment use and fertilizer production. In their work, it was the pasture midwest system that was found to be associated with the greatest long-term warming, beating midwest feedlots. These authors also noted that in many cases, like in the pasture midwest system, there are still considerable emissions coming from farm equipment, fertilization, and feed production, as well as high methane emissions. It was the grain-fed ranch system in Sweden that was found to contribute the least to long-term warming. [26].

However, it is important to emphasize that when comparing grass- and grain-finished systems using the CO_2e metric, we see a significantly greater warming effect under grass-finishing. Moreover, the CO_2e metric

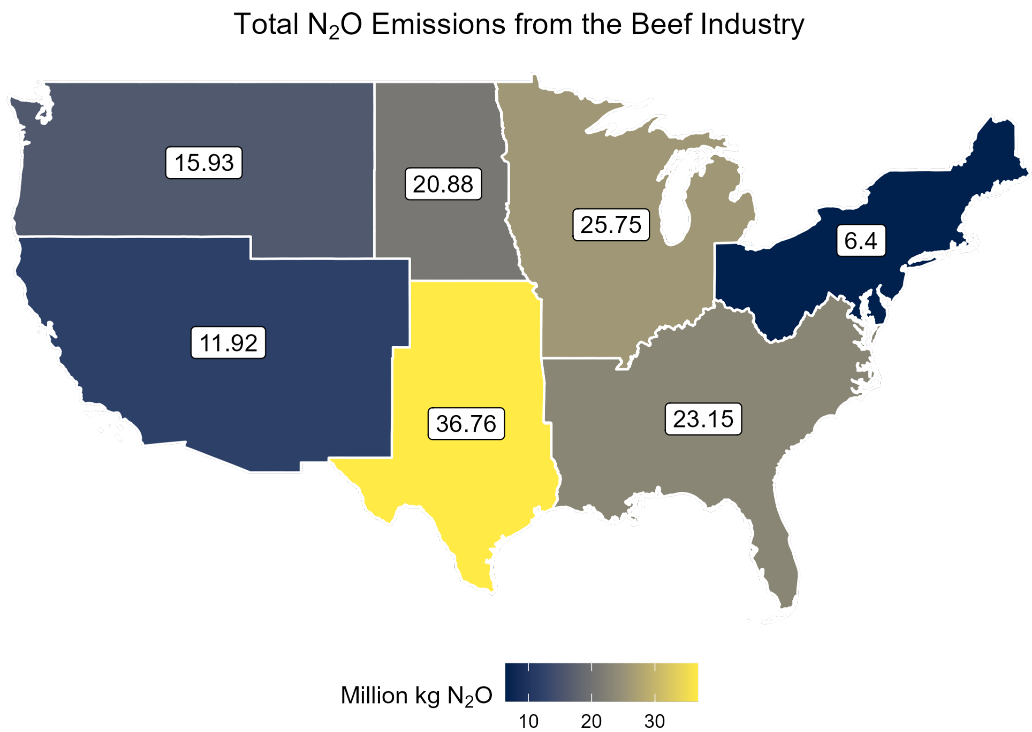

Figure 9: Predicted total N_2O emissions for the beef cattle industry

implies that methane is primarily responsible for warming in both systems, whereas our results indicate that N_2O is dominant.

In this work we have used only a single point estimate for all parameters, many of which are uncertain or variable. For example, many of the feed characteristics summarized in Table 4 are variable based on region, the type of corn grain being fed to the cattle, or type of grass that cattle grazed on. Emissions of all gases at different cattle life cycle stages may also vary appreciably. Thus, doing a sensitivity analysis on many of our parameters, across a range of possible values would better represent the possible range of climate outcomes. Moreover, more precise regional values of parameters were also largely unconsidered, aside from methane conversion factors and farm operation CO_2 emissions. Dairy cattle were completely left out of our emissions flow, despite the large contribution they make to cattle industry GHG emissions in the US, and the non-trivial contribution of dairy culls to beef production [32]. Future work should thus focus on better representing the intrinsic and regional variability in the US cattle industry and GHG emissions, and

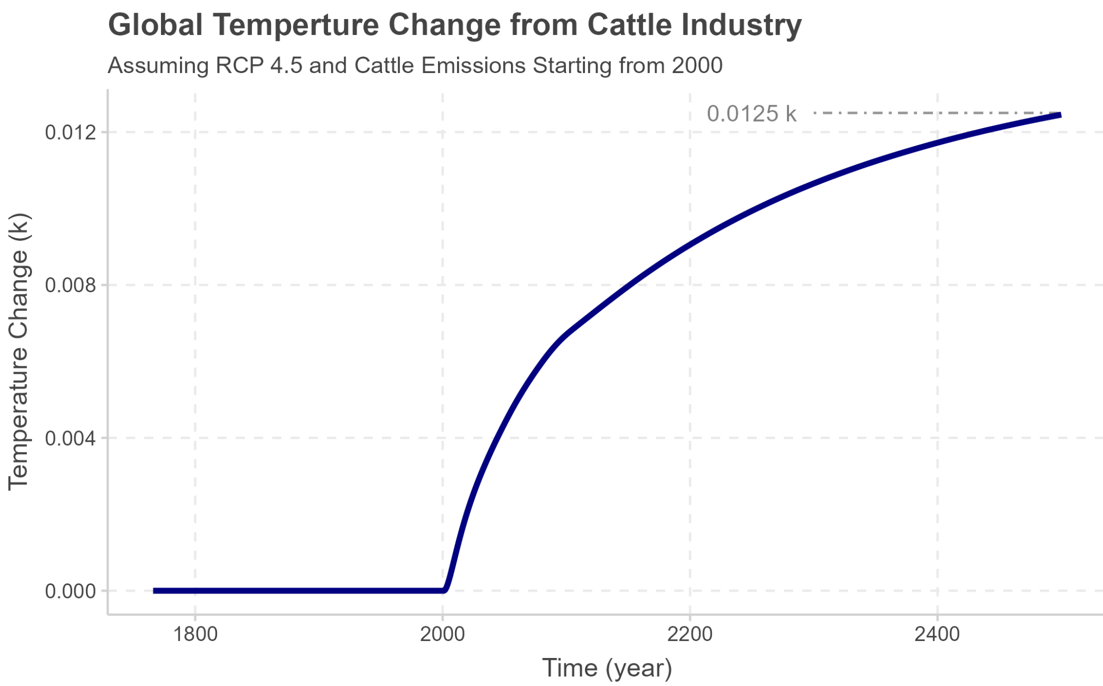

Figure 10: Total temperature change attributed to the model beef system

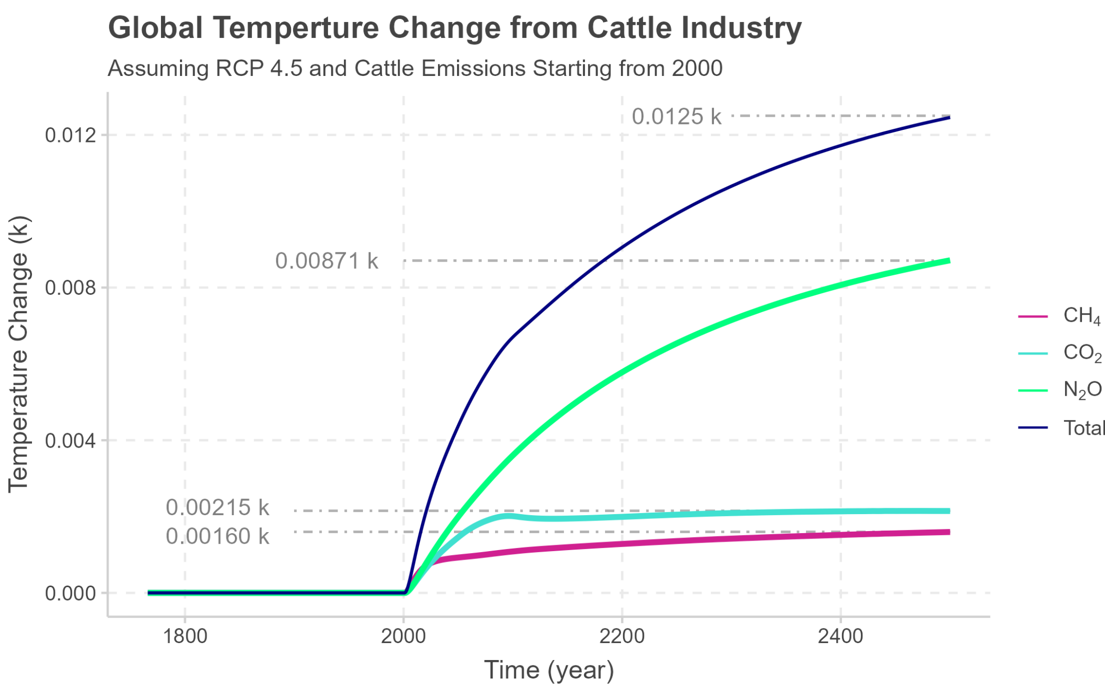

Figure 11: Temperature change by greenhouse gas

evaluating the sensitivity of our conclusions to uncertainty in these parameters.

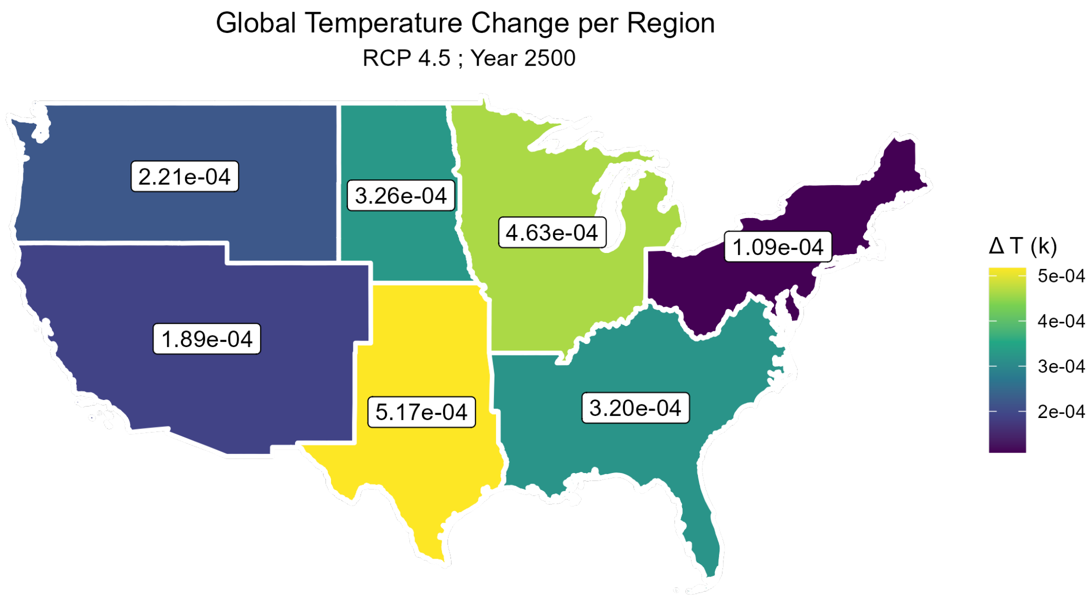

Figure 12: Temperature change attributed to Each U.S. Region

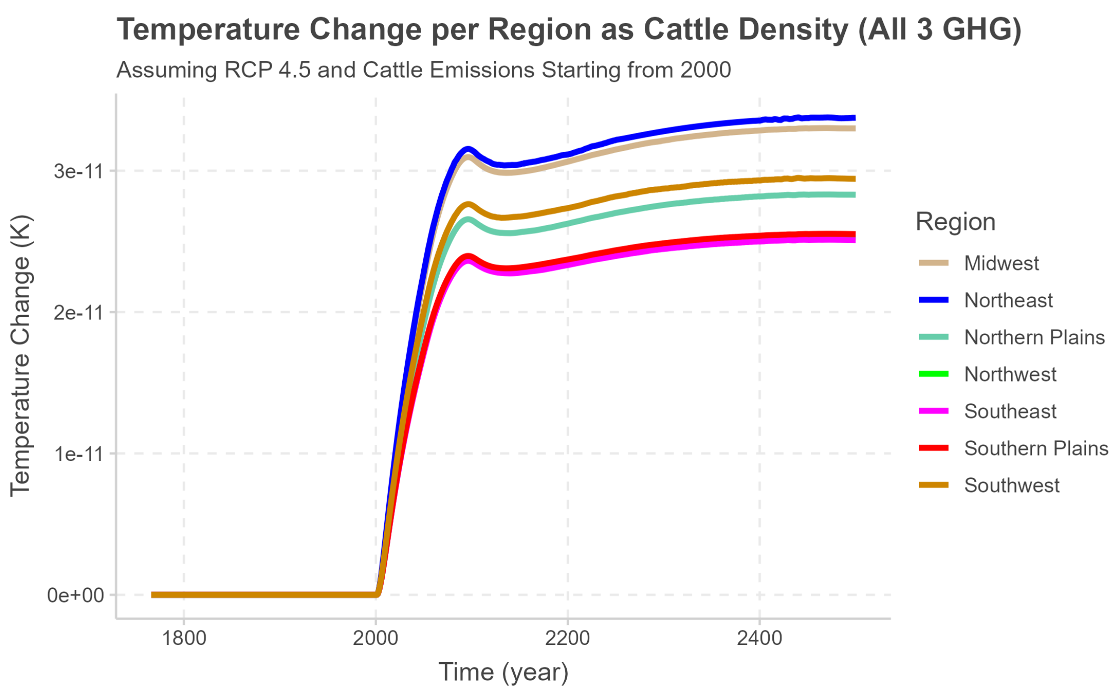

Figure 13: Temperature Change per Region (All 3 GHG) and Temperature Change per Region in terms of temperature change per head.

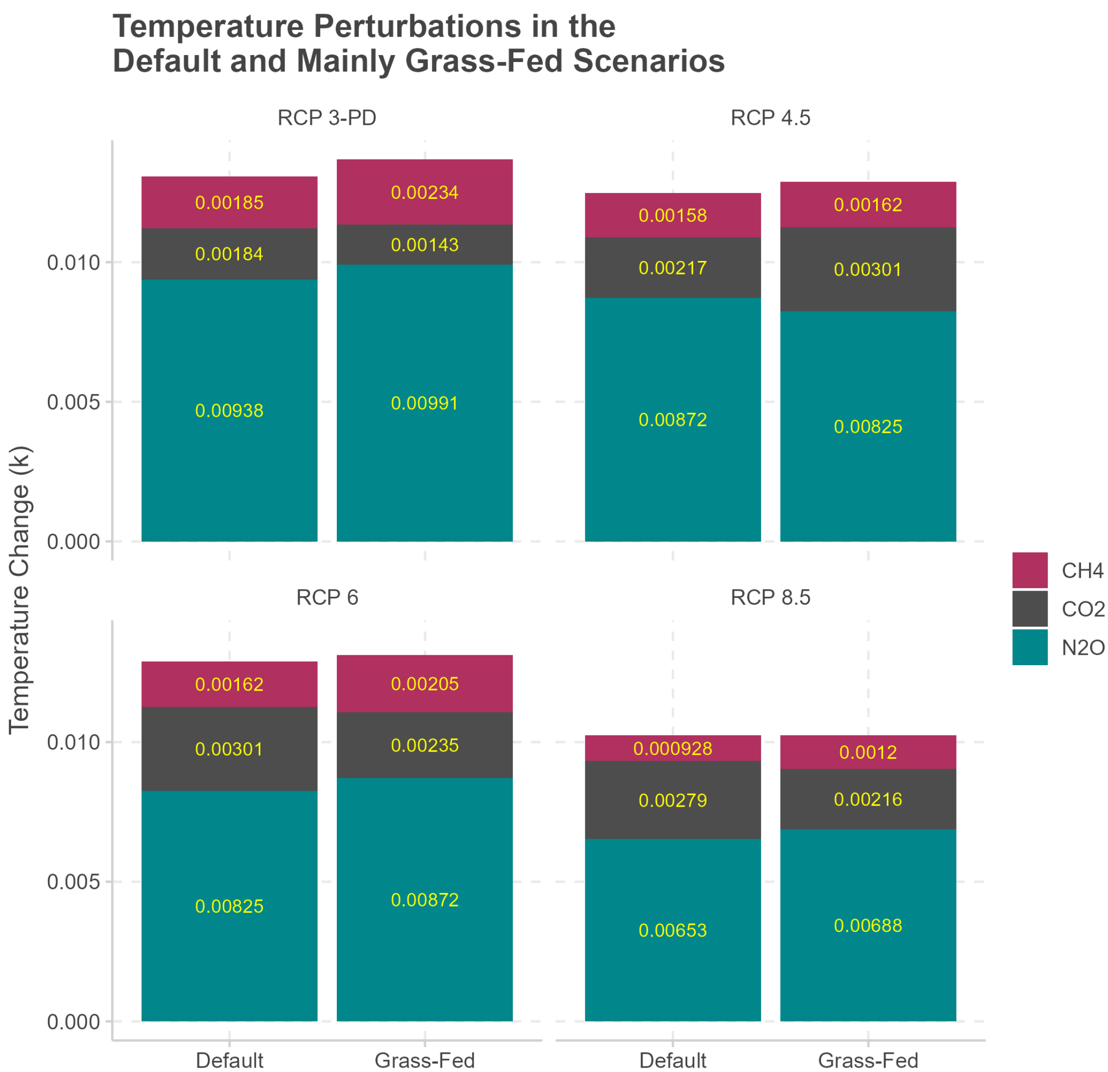

Figure 14: Temperature change attributable to each gas under the default beef herd and a primarily grass-finished beef herd, for each background RCP.

In addition to the majority grain-finished vs. grass-finished model herds we have compared, future research should look at additional alternative herd makeups, which can be simulated by our cattle life cycle model, to see if alternative production practices may be more sustainable. Additionally, because of our finding that N_2O contributes to the majority of warming at the 500-year timescale, further research should go into the feasibility of reducing nitrous oxide emissions from fertilizer and manure management. Mitigation of all greenhouse gas emissions is important, especially CO_2 emissions, since warming from these emissions are essentially fixed for hundreds of thousands of years. However, if the goal is to decrease warming from the cattle industry over the next 500 years, our model suggests focusing on the mitigation of N_2O as opposed to methane, despite the higher concentrations of methane released by beef cattle each year.

Overall, the global temperature perturbation attributable to the US beef industry was about 0.0125 K in the year 2500. Although a warming effect of 0.0125 K may not seem like a large temperature increase in

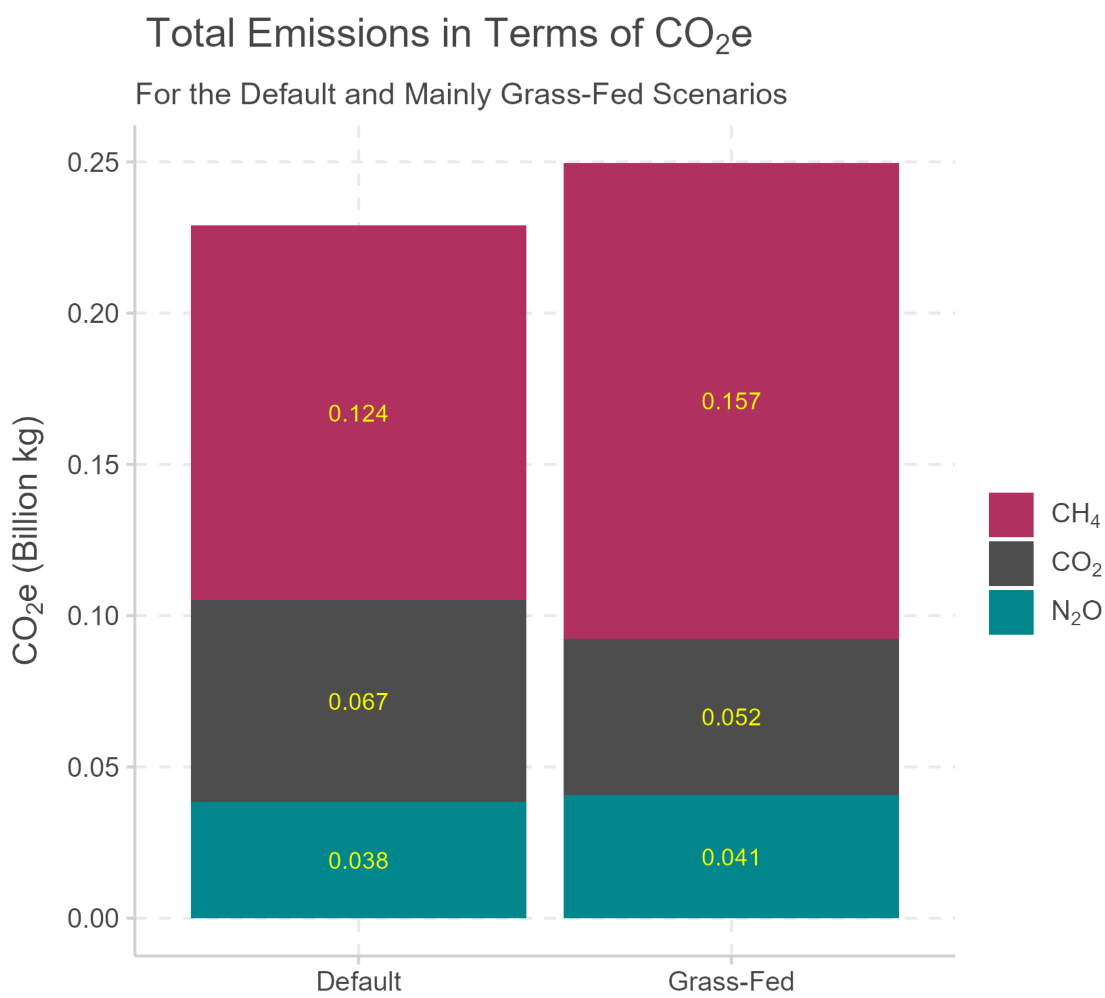

Figure 15: Total beef industry emissions from default and mainly grass-fed scenarios in terms of CO_2e

general, we need to bear in mind that this increase comes from only the beef cattle in the United States. It does not include dairy cattle, it does not include agricultural emissions from other systems, it does not include emissions from the entire United States, and it does not touch emissions coming from the rest of the world. This is a very narrow category of operations that is contributing to a non-negligible increase. Thus, GHG mitigation is essential in the US beef industry.

5 Conclusion

Our models predict the global temperature increase, due solely to the beef industry in the United States, to be approximately 0.0125 K at the year 2500 primarily due to nitrous oxide emissions coming from cattle manure and fertilizer use. This is contrary to the current emphasis placed on methane emissions from the more commonly used CO_2 equivalent metric. Our models also showed that grass-finished beef produced only marginally more long-term warming than grain-finished beef. This is in contrast to the CO_2e metric, which predicts higher warming from grass-fed beef than our model. We have demonstrated, as well as past literature, that warming is better captured by models like ours, which look at the temperature change associated with individual greenhouse gases. This suggests that steps to mitigate emissions from agriculture should target nitrous oxide production. To prepare for and mitigate future climate catastrophe, we need to understand what is contributing to long-term warming: Modelling emissions and warming from the cattle industry is our small contribution to this goal. "So often the end of a love affair is death by a thousand cuts, so often its survival is life by a thousand stitches" (Robert Breault).

References

[1] Accessed on: 2024-07-04. URL: https://www.naturesseed.com/pasture-seed/cattle-pastures/beef-cattle-forage/southwest-desert-beef-cattle-forage-mix/.

[2] Myles R Allen et al. "A solution to the misrepresentations of CO2-equivalent emissions of short-lived climate pollutants under ambitious mitigation". In: *Npj Climate and Atmospheric Science* 1.1 (2018), p. 16.

[3] *ANNUAL CROP SUMMARY - 2022*. [Accessed 16-07-2024]. URL: https://www.nass.usda.gov/Statistics_by_State/Wyoming/Publications/News_Releases/2023/WY-Crop-Production-01122023.pdf.

[4] Senorpe Asem-Hiablie et al. "A life cycle assessment of the environmental impacts of a beef system in the USA". In: *The International Journal of Life Cycle Assessment* 24 (2019), pp. 441–455.

[5] Senorpe Asem-Hiablie et al. "Management characteristics of beef cattle production in the western United States". In: *The Professional Animal Scientist* 33.4 (2017), pp. 461–471.

[6] Hannah Bäck et al. "Effect of methane mitigation on global temperature under a permafrost feedback". In: *Global Environmental Change Advances* 2 (2024), p. 100005.

[7] *Corn Silage*. [Accessed 18-07-2024]. URL: https://extension.illinois.edu/beef-cattle/corn-silage#:~:text=To%20achieve%20this%20goal%2C%20the,of%2065%25)%20for%20chopping..

[8] Ciniro Costa et al. "Global Warming Potential*(GWP*): Understanding the implications for mitigating methane emissions in agriculture". In: (2021).

[9] P Crosson et al. "A review of whole farm systems models of greenhouse gas emissions from beef and dairy cattle production systems". In: *Animal Feed Science and Technology* 166 (2011), pp. 29–45.

[10] S. Dhakal et al. "Emissions Trends and Drivers". In: *Climate Change 2022: Mitigation of Climate Change. Contribution of Working Group III to the Sixth Assessment Report of the Intergovernmental Panel on Climate Change*. Ed. by P.R. Shukla et al. Cambridge, UK and New York, NY, USA: Cambridge University Press, 2022. Chap. 2. DOI: 10.1017/9781009157926.004. URL: https://www.ipcc.ch/report/ar6/wg3/downloads/report/IPCC_AR6_WGIII_Chapter02.pdf.

[11] Maryam Etminan et al. "Radiative forcing of carbon dioxide, methane, and nitrous oxide: A significant revision of the methane radiative forcing". In: *Geophysical Research Letters* 43.24 (2016), pp. 12–614.

[12] *Fertilizing Hay and Pastures — Agronomic Crops Network — agcrops.osu.edu*. [Accessed 18-07-2024]. URL: https://agcrops.osu.edu/newsletter/corn-newsletter/16-2021/fertilizing-hay-and-pastures#:~:text=Moderate%20amounts%20of%20nitrogen%20(30,grasses%20are%20over%20in%20pastures.

[13] Michael Gibbs, Paul Jun, and Kathryn Gaffney. *CH4 and N2O emissions from livestock manure*. Accessed on: 2024-07-04. 2003. URL: https://www.ipcc-nggip.iges.or.jp/public/gp/bgp/4_2_CH4_and_N2O_Livestock_Manure.pdf.

[14] Michael J Gibbs et al. *CH4 emissions from enteric fermentation*. Accessed on: 2024-07-04. 2003. URL: https://www.ipcc-nggip.iges.or.jp/public/gp/bgp/4_1_CH4_Enteric_Fermentation.pdf.

[15] Michael J Glotter et al. "A simple carbon cycle representation for economic and policy analyses". In: *Climatic Change* 126 (2014), pp. 319–335.

[16] Corinne A Hartin et al. "A simple object-oriented and open-source model for scientific and policy analyses of the global climate system–Hector v1. 0". In: *Geoscientific Model Development* 8.4 (2015), pp. 939–955.

[17] KR Heflin et al. "Greenhouse-gas emissions of beef finishing systems in the Southern High Plains". In: *Agricultural Systems* 176 (2019), p. 102674.

[18] John Lynch et al. "Agriculture's contribution to climate change and role in mitigation is distinct from predominantly fossil CO2-emitting sectors". In: *Frontiers in sustainable food systems* 4 (2021), p. 518039.

[19] M Meinshausen. *RCP Concentration Calculations and Data Final Version, background data, acknowledgements and further info.* Accessed on: 2024-07-04. 2011.

[20] Malte Meinshausen, Sarah CB Raper, and Tom ML Wigley. "Emulating coupled atmosphere-ocean and carbon cycle models with a simpler model, MAGICC6–Part 1: Model description and calibration". In: *Atmospheric Chemistry and Physics* 11.4 (2011), pp. 1417–1456.

[21] Malte Meinshausen et al. "The RCP greenhouse gas concentrations and their extensions from 1765 to 2300". In: *Climatic change* 109 (2011), pp. 213–241.

[22] C Morice et al. "Met Office Hadley Centre observations datasets". In: *can be found under https://www. metoffice. gov. uk/hadobs/hadcrut4/index. html* (2016).

[23] Aditi Mukherji. "Climate Change 2023 Synthesis Report". In: (2023).

[24] Nathan Pelletier, Rich Pirog, and Rebecca Rasmussen. "Comparative life cycle environmental impacts of three beef production strategies in the Upper Midwestern United States". In: *Agricultural Systems* 103.6 (2010), pp. 380–389.

[25] Ramond T Pierrehumbert. "Short-lived climate pollution". In: *Annual review of earth and planetary sciences* 42 (2014), pp. 341–379.

[26] RT Pierrehumbert and G Eshel. "Climate impact of beef: an analysis considering multiple time scales and production methods without use of global warming potentials". In: *Environmental Research Letters* 10.8 (2015), p. 085002.

[27] Joseph Poore and Thomas Nemecek. "Reducing food's environmental impacts through producers and consumers". In: *Science* 360.6392 (2018), pp. 987–992.

[28] Michael J Prather et al. "Measuring and modeling the lifetime of nitrous oxide including its variability". In: *Journal of Geophysical Research: Atmospheres* 120.11 (2015), pp. 5693–5705.

[29] *Protein Supplementation in Corn Silage-Based Diets – A Review — beef.unl.edu.* [Accessed 18-07-2024]. URL: https://beef.unl.edu/beefwatch/2022/protein-supplementation-corn-silage-based-diets-%E2%80%93-review.

[30] *Reading a Forage Analysis Report.* [Accessed 16-07-2024]. URL: https://afs.ca.uky.edu/content/reading-forage-analysis-report#:~:text=Dry%20hay%20generally%20contains%2088,8%20to%2012%25%20moisture.

[31] Andy Reisinger and Harry Clark. "How much do direct livestock emissions actually contribute to global warming?" In: *Global change biology* 24.4 (2018), pp. 1749–1761.

[32] C Alan Rotz et al. "Environmental footprints of beef cattle production in the United States". In: *Agricultural systems* 169 (2019), pp. 1–13.

[33] George Smeeton. *Net zero: Why is it necessary?* Sept. 2018. URL: https://eciu.net/analysis/briefings/net-zero/net-zero-why#:~:text=Climate%20science%20is%20clear%20that,need%20to%20fall%20to%20zero.

[34] Christopher J Smith et al. "FAIR v1. 3: a simple emissions-based impulse response and carbon cycle model". In: *Geoscientific Model Development* 11.6 (2018), pp. 2273–2297.

[35] Keith Smith, Lex Bouwman, and Barbara Braatz. *N2O: Direct Emissions From Agricultural Soils*. Accessed on: 2024-07-04. 2001. URL: https://www.ipcc-nggip.iges.or.jp/public/gp/bgp/4_5_N2O_Agricultural_Soils.pdf.

[36] Clifford S Snyder et al. "Review of greenhouse gas emissions from crop production systems and fertilizer management effects". In: *Agriculture, Ecosystems & Environment* 133.3-4 (2009), pp. 247–266.

[37] *Timothy (Phleum pratense), hay*. Accessed on: 2024-07-16. URL: https://www.feedipedia.org/node/16888.

[38] *Understanding Global Warming Potentials — US EPA — epa.gov*. https://www.epa.gov/ghgemissions/understanding-global-warming-potentials. [Accessed 11-07-2024].

[39] *Understanding your hay analysis*. Accessed on 2024-07-15. URL: https://extension.umn.edu/horse-nutrition/understanding-your-hay-analysis#crude-protein-%28cp%29-1320261.

[40] USDA. *Crop production - 2023 summary January 2024*. Accessed on: 2024-07-15. Jan. 2024. URL: https://downloads.usda.library.cornell.edu/usda-esmis/files/k3569432s/ns065v292/8910md644/cropan24.pdf.

[41] US USDA. "Fertilizer use and price". In: *US Department of Agriculture, Economic Research Service* (2019).

[42] Heuzé V. et al. *Bermuda grass (Cynodon dactylon)*. Accessed on: 2024-07-04. URL: https://www.feedipedia.org/node/471.

[43] Sonja J Vermeulen, Bruce M Campbell, and John SI Ingram. "Climate change and food systems". In: *Annual review of environment and resources* 37 (2012), pp. 195–222.